University of Alberta

Characterizations of Polyethyleneimine-Plasmid DNA Complexes for Gene Delivery

by

Weinan Hu

A thesis submitted to the Faculty of Graduate Studies and Research
in partial fulfillment of the requirements for the degree of

Master of Science
in
Chemical Engineering

Department of Chemical and Materials Engineering

Edmonton, Alberta
Spring 2008

Library and Archives Canada

Published Heritage Branch

395 Wellington Street
Ottawa ON K1A 0N4
Canada

Bibliothèque et Archives Canada

Direction du Patrimoine de l'édition

395, rue Wellington
Ottawa ON K1A 0N4
Canada

Your file Votre référence
ISBN: 978-0-494-45825-9
Our file Notre référence
ISBN: 978-0-494-45825-9

NOTICE:
The author has granted a non-exclusive license allowing Library and Archives Canada to reproduce, publish, archive, preserve, conserve, communicate to the public by telecommunication or on the Internet, loan, distribute and sell theses worldwide, for commercial or non-commercial purposes, in microform, paper, electronic and/or any other formats.

The author retains copyright ownership and moral rights in this thesis. Neither the thesis nor substantial extracts from it may be printed or otherwise reproduced without the author's permission.

AVIS:
L'auteur a accordé une licence non exclusive permettant à la Bibliothèque et Archives Canada de reproduire, publier, archiver, sauvegarder, conserver, transmettre au public par télécommunication ou par l'Internet, prêter, distribuer et vendre des thèses partout dans le monde, à des fins commerciales ou autres, sur support microforme, papier, électronique et/ou autres formats.

L'auteur conserve la propriété du droit d'auteur et des droits moraux qui protège cette thèse. Ni la thèse ni des extraits substantiels de celle-ci ne doivent être imprimés ou autrement reproduits sans son autorisation.

In compliance with the Canadian Privacy Act some supporting forms may have been removed from this thesis.

While these forms may be included in the document page count, their removal does not represent any loss of content from the thesis.

Conformément à la loi canadienne sur la protection de la vie privée, quelques formulaires secondaires ont été enlevés de cette thèse.

Bien que ces formulaires aient inclus dans la pagination, il n'y aura aucun contenu manquant.

Canada

ABSTRACT

Non-viral vectors such as cationic polymers are widely used in gene therapy researches. Upon interaction with cationic polymers, DNA was condensed and neutralized to form complex for gene delivery. In this study, we focused on characterizing some important biophysical properties of the cationic polymer/DNA complexes, such as zeta potential, zeta potential distribution, particle size and particle shape utilizing Zetasizer and AFM. The effects of ionic strength and pH value of the solution on complexation were also investigated. We concluded that high ionic strength adversely affected the binding between cationic polymer and DNA, and promoted aggregation. We also established a correlation between zeta potential of the system and the particle size. A kinetic study with AFM illustrated the complex formation process and the interaction between DNA molecules and cationic polymers. Complex formation occurred within 10 minutes upon mixing and completed after 20-30 minutes.

ACKNOWLEDGEMENTS

First of all, I would like to express my gratitude to my supervisors, Dr. Hasan Uludag and Dr. Zhenghe Xu, for their insightful guidance, constructive advice, and most of all, their patience and understanding. I would also like to gratefully acknowledge Natural Sciences and Engineering Research Council of Canada (NSERC) for financial support.

I would like to thank Dr. Afsaneh Lavasanifar for her time and energy devoted to review my thesis, and her fresh perspective on the work. My gratitude also goes to Dr. Janet Elliot for her time and support before and during the thesis defence.

I would like to express my thanks to Cezary Kucharski for preparing the linear DNA, Basak Acan-Clements for preparing the pEGFP-N2 and Dr. Jiang Bai for helping the preparation of PEI for this study. Expert technical help of Dr. Jianjun Liu, Dr. Dengli Qiu and Dr. Li-yan Zhang with atomic force microscope are very much appreciated. I would also like to take this opportunity to thank all the people in my research group for their valuable advice.

I am deeply indebted to my wife, Mei Huang, for her continuous love, immeasurable support and eminent understanding throughout the years. I would also like to express my special thanks to my loving parents for always believing in me. No words can show my deepest appreciation towards them.

Finally but immensely, I would like express my highest gratitude to my grandfather, Dr. Jin Chen. Without your encouragement and inspiration, none of these is possible. May you rest in heaven.

TABLE OF CONTENTS

1. INTRODUCTION **1**

1.1 Gene Therapy 1

1.2 Cationic Polymers as Gene Carrier 3

1.3 Complex Formation 7

1.4 Particle Size 10

1.5 Transfection Efficiency 11

1.6 Zeta Potential 13

1.7 Photon Correlation Spectroscopy (PCS) 16

1.8 Atomic Force Microscopy (AFM) 17

2. SCOPE **21**

3. MATERIALS AND METHODS **23**

3.1 Materials 23

3.2 Analysis by Zetasizer 25

3.2.1 Zeta Potential Analysis 25

3.2.1.1 Complex Formation 25

3.2.1.1.1 PEI/PAA Complexes 25

3.2.1.1.2 PEI/Linear DNA 26

3.2.1.2 Zeta Potential Measurement 29

3.2.2 Zeta potential Distribution Analysis 30

3.2.3 Photon Correlation Spectroscopy (PCS) 30

3.3 Analysis by Atomic Force Microscopy 33

3.3.1 Imaging of PEI/Linear DNA Complexes Under AFM 33

3.3.2 Imaging Naked Plasmid DNA Under AFM 34

3.3.3 Investigation of Complex Formation Under AFM 34

3.3.4 Imaging PEI/Plasmid DNA Complexes Under AFM 35

4. RESULTS **36**

4.1 Zeta Potential Analysis 36

4.1.1 PEI/PAA Complexes in H_2O 36

4.1.2 PEI/Linear DNA Complexes in H_2O 38

4.1.3 PEI/Linear DNA Complexes in NaCl Solution 40

4.1.4 PEI/Linear DNA Complexes in Phosphate Buffer 42

4.2 Zeta Potential Distribution 46

4.3 Size Measurement 49

4.3.1 PEI/PAA Complexes in H_2O 49

4.3.2 PEI/Linear DNA Complexes in H_2O 51

4.3.3 PEI/Linear DNA Complexes in NaCl Solution 53

4.3.4 PEI/Linear DNA Complexes in Phosphate Buffer 55

4.4 AFM Imaging

4.4.1 Correlation of AFM Imaging and PCS 60

4.4.2 AFM Imaging of Plasmid DNA 64

4.4.3 Investigation of Complex Formation under AFM 66

4.4.4 AFM Imaging of PEI/Plasmid DNA Complexes in 3 mM NaCl 68

5. DISCUSSION **72**

6. CONCLUSIONS 79

7. FUTURE PROSPECTS 81

8. REFERENCES 83

LIST OF FIGURES

Figure 1-1.	The structure of cationic polymers studied as gene carriers.	**6**
Figure 1-2.	Illustration of the non-viral gene delivery multistep process.	**8**
Figure 1-3.	Illustration of the concept of Stern layer, diffuse layer, slipping plane and zeta potential.	**15**
Figure 1-4.	An illustration of the AFM operation.	**18**
Figure 2-1.	The restriction map and multiple cloning site of pEGFP-N2.	**24**
Figure 3-1.	The average zeta potential of PEI/PAA complexes as a function of PEI/PAA mass ratio.	**38**
Figure 3-2.	The average zeta potential of PEI/linear DNA complexes in H_2O as a function of PEI/linear DNA mass ratio.	**39**
Figure 3-3.	The average zeta potential of PEI/linear DNA complexes in NaCl buffers (30 mM and 150 mM) as a function of PEI/linear DNA mass ratio.	**42**
Figure 3-4A.	The average zeta potential of PEI/linear DNA complexes in phosphate buffers with different pH values (5.0, 6.0, 7.0 and 8.0, NaCl concentration was 30 mM) as a function of PEI/linear DNA mass ratio.	**44**
Figure 3-4B.	The average zeta potential of PEI/linear DNA complexes in phosphate buffers with different pH values (5.0 and 6.0, NaCl concentration was 150 mM) as a function of PEI/linear DNA mass ratio.	**45**
Figure 3-5.	The zeta potential distributions for PEI/linear DNA complexes at pH 5.0 in 30 mM NaCl solution.	**47**
Figure 3-6.	The average size of PEI/PAA complexes in H_2O as a function of PEI/PAA mass ratio.	**50**
Figure 3-7.	The average size of PEI/linear DNA complexes in H_2O as a function of PEI/linear DNA mass ratio.	**52**
Figure 3-8.	The average size of PEI/linear DNA complexes in NaCl as a function of PEI/DNA mass ratio.	**55**

Figure 3-9A. The average size of PEI/linear DNA complexes in phosphate buffers with different pH values (NaCl concentration was 30 mM) as a function of PEI/linear DNA mass ratio. **58**

Figure 3-9B. The average size of PEI/linear DNA complexes in phosphate buffers with different pH values (NaCl concentration was 150 mM) as a function of PEI/DNA mass ratio. **60**

Figure 3-10. AFM images of PEI/linear DNA complexes in H_2O at different PEI/DNA mass ratios. **62**

Figure 3-11. The average size of PEI/linear DNA complexes obtained from AFM images at different mass ratio in H_2O. **63**

Figure 3-12. AFM images of plasmid DNA (pEGFP). **65**

Figure 3-13. AFM images of PEI/DNA complexes at different complexation time. **66**

Figure 3-14. AFM images of PEI/plasmid DNA complexes in 3 mM NaCl at different PEI/plasmid DNA mass ratios. **70**

Figure 3-15. The average size of PEI/plasmid DNA complexes at different mass ratio in 3mM NaCl. **71**

LIST OF TABLES

Table 1-1. Comparison of AFM with other microscopy techniques: TEM, SEM and optical microscopy. **19**

Table 2-1. The concentration of PEI and PAA used for PEI/PAA complex zeta potential measurements. **26**

Table 2-2A. The concentration of PEI and DNA used for PEI/DNA complex zeta potential measurements in H_2O. **27**

Table 2-2B. The concentration of PEI and DNA used for PEI/DNA complex zeta potential measurements in NaCl buffers (30mM and 150 mM). **27**

Table 2-2C. The concentration of PEI and DNA used for PEI/DNA complex zeta potential measurements in phosphate buffer at different pH with NaCl concentration of 30 mM. **28**

Table 2-2D. The concentration of PEI and DNA used for PEI/DNA complex zeta potential measurements in phosphate buffer at different pH with NaCl concentration of 150 mM. **28**

Table 2-3. The concentration of PEI and PAA used for PEI/PAA complex particle size measurements. **30**

Table 2-4A. The concentration of PEI and DNA used for PEI/DNA complex particle size measurements in H_2O. **31**

Table 2-4B. The concentration of PEI and DNA used for PEI/DNA complex particle size measurements in NaCl buffers. **31**

Table 2-4C. The concentration of PEI and DNA used for PEI/DNA complex particle size measurements in phosphate buffer at different pH with NaCl concentration of 30 mM. **32**

Table 3-1. The characteristic of PEI/PAA samples used for zeta potential measurements and the obtained zeta potential values of the PEI/PAA complexes. **37**

Table 3-2. The characteristic of PEI/linear DNA samples used for zeta potential measurements and the obtained average zeta potential values of the PEI/linear DNA complexes. **39**

Table 3-3. The characteristic of PEI/linear DNA samples used for zeta potential measurements and the obtained average zeta potential values of the PEI/linear DNA complexes in NaCl. **41**

Table 3-4A. The characteristic of PEI/linear DNA samples used for zeta potential measurements and the obtained average zeta potential values of the PEI/linear DNA complexes in phosphate buffer (NaCl conc. =30 mM). **43**

Table 3-4B. The characteristic of PEI/linear DNA samples used for zeta potential measurements and the obtained average zeta potential values of the PEI/linear DNA complexes in phosphate buffer (NaCl conc. =150 mM). **45**

Table 3-5. The characteristic of PEI/PAA samples used for size measurements and the obtained average size of the PEI/PAA complexes in H_2O. **49**

Table 3-6. The characteristic of PEI/linear DNA samples used for size measurements and the obtained average size of the PEI/linear DNA complexes in H_2O. **51**

Table 3-7. The characteristic of PEI/linear DNA samples used for size measurements and the obtained average size of the PEI/linear DNA complexes in NaCl. **54**

Table 3-8A. The characteristic of PEI/linear DNA samples used for size measurements and the obtained average size of the PEI/linear DNA complexes in phosphate buffer (NaCl conc. =30 mM). **57**

Table 3-8B. The characteristic of samples used for size measurements and the obtained average size of the PEI/linear DNA complexes in phosphate buffer (NaCl conc. =150 mM). **59**

Table 3-9. The AFM results of the size of PEI/linear DNA complexes in H_2O. **61**

Table 3-10. The AFM results of the size of PEI/plasmid DNA complexes in 3mM NaCl. **69**

ABBREVIATIONS

PLL:	Poly-(L-lysine)
PEI:	Polyethyleneimine
PAMAM:	Polyamidoamine
PLA:	Poly-(L-arginine)
DSC:	Differential Scanning Calorimetry
EM:	Electron Microscope
AFM:	Atomic Force Microscope
FTIR:	Fourier Transform Infrared
N/P:	Nitrogen-to-Phosphate
DNase I:	Deoxyribonuclease I
bp:	Base Pair
kbp:	Kilo Base Pair
PCS:	Photon Correlation Spectroscopy
DLS:	Dynamic Light Scattering
SPM:	Scanning Probe Microscope
STM:	Scanning Tunneling Microscope
SEM:	Scanning Electron Microscope
TEM:	Transmission Electron Microscope
PAA:	Poly (Acrylic Acid)

1. INTRODUCTION

Genes are the basic physical and functional units of heredity. They are sequences of bases that encode the information for making specific proteins. Proteins are essential to the structure and function of all living cells. A gene is altered as such that encoded proteins are not able to carry out their normal functions, genetic disorders can occur. More than 6000 diseases are known to be caused by a single gene defect. Conventional medicine sometimes can only control the symptoms, but cures are out of reach.

1.1 Gene Therapy

Gene therapy is a medical treatment that delivers a gene into cells in order to produce their own therapeutic proteins that change the function of those cells. The goal of gene therapy is to substitute a defective gene by a healthy one, or to repair a faulty gene. Delivering functional gene into the selected cell is the essential step in the procedure of gene therapy. Currently there are two major groups of vectors for gene delivery, viral vectors and non-viral vectors. They both have their intrinsic advantages and disadvantages.

Viral vectors, such as retroviruses and adenoviruses are commonly used in gene delivery since the molecular biology of recombinant viruses is well understood. Viral vectors are well investigated because of their high transfection efficiency. However, disadvantages of viral vectors for gene transfer limited their application. For instance, the risk of host immunological responses to the viral particle is one of the toughest challenges. This will likely prevent repeated *in vivo* transfection using the same vector

[1]. At the same time, there are also toxicity and safety concerns regarding the use of viral vector. Though random recombination with wild-type viruses were not reported, it is theoretically possible. In addition, the size of DNA that can be transported by viral vectors is usually limited, not to mention the lack of cell type specificity of the viral gene delivery system and the potential high cost.

Non-viral approaches in gene delivery hold great promise as an alternative. Generally speaking, non-viral methods can be divided into two major categories: physical and chemical. Physical means include delivering plasmid DNA to cells by electroporation, sonication, or particle bombardment [2-4]. Chemical methods on the other hand, introduce synthetic vectors that will complex with DNA, condense it into particles and direct it to the cells. These non-viral vectors are mostly cationic, have high amine ratios, and can not only bind DNA into condensed particles but also neutralize the charge of the complex, allowing easy transporting through cell membranes which are negatively charged. However, the transfection efficiency for non-viral gene delivery systems is comparatively much lower than viral vectors, especially *in vivo*. Despite their drawbacks, interests in developing non-viral gene delivery have been constantly growing due to their advantageous safety profile. Non-viral gene delivery systems have shown promising results in circumventing toxicity and immunogenecity in gene delivery process. Compared to their viral counterparts, non-viral vectors are normally easier and less expensive to manufacture and can be obtained on a much larger scale. They also have the potential to transfect cells with larger pieces of genetic materials than adenoviral transfection methods [5]. In addition, due to their synthetic nature, non-viral vectors can

also be specifically modified for the proposed application on molecular level and highly purified afterwards.

Non-viral vectors mainly include cationic lipids, such as Lipofectin (Invitrogen Corp.), Transfectam (Promega Corp.), Lipofectase (Gibco-BRL), Lipofectamine (Invitrogen Corp.), and LipoTaxi (Stratagene Corp.), as well as cationic polymers and peptides (e.g. PLL, PEI, PAMAM dendrimers, etc.). Cationic lipids are amphiphilic molecules containing a positively charged polar headgroup linked to a hydrophobic domain. Due to their amphiphilic characteristic, they are able to self-assemble into liposome and somehow encapsulate the condensed DNA to form lipoplexes upon mixing [6]. Although cationic lipid-based gene carriers are currently evaluated clinically to higher extent than polyplexes, synthetic cationic polymers were reported to be superior to cationic lipids *in vitro* because they can also promote gene delivery from the cytoplasm to the nucleus and they would not block plasmid DNA's transgene expression after complexation.

1.2 Cationic Polymers as Gene Carrier

The development of cationic polymers as gene delivery agents has seen rapid advances for the past twenty years [7]. Cationic polymers generally contain high densities of primary, secondary, tertiary or quaternary amines. This high density of positive charges allows the cationic polymers to complex with negatively charged DNA and form relatively stable polyplexes. The structural characteristics of these cationic polymers are widely varied, ranging from linear to highly branched chains. Moreover, the deposition of the positive charges on the polymers is different. Some cationic polymers have the positive charges on the backbone while others are on side groups.

These factors will influence their complexation with nucleic acids and their transfection efficiency. Given their polymeric nature, cationic polymers are remarkably valuable for gene delivery studies. They can not only be synthesized in different lengths with different geometry, but also specifically tailored with substitution or addition of functional groups. All of these features will be essential for studies on structure/function relationship of non-viral vectors.

PLL (Figure 1-1A) and PLA were some of the first generation of cationic polymers developed for gene delivery applications [8, 9]. The lack of a hydrophobic domain in structure limited their ability to interact with the endosomal membrane in order to fuse/destabilize the endosome. Hence, their transfection efficiency was considerably low because of the ineffectual endosomal escape. However, the fact that positively charged PLL contains high density of primary amines has led to the development of strategies that enhance the endosomal destabilization ability of polyplexes. In addition to providing positive charges for DNA complexation, the primary amines of PLL can also serve as functional groups to covalently link the polymers with ligands and peptides for enhancing the endosome-disrupting properties [10-12]. Actually, PLL is arguably the most widely used cationic polymer for attaching targeting ligands in receptor-mediated gene delivery because of the high density of primary amines, despite the fact that the chain length heterogeneity of the commercially available PLL will inevitably complicate the kinetics of the PLL/DNA interaction, the thermodynamic stability and size distribution of the final polyplexes.

Dendrimers are another type of cationic polymers as candidates for gene carriers. Different from PLL and other classical polymers, dendrimers are known for their high

degree of molecular uniformity, narrow molecular weight distribution, specific size and shape characteristics, and a highly functionalized terminal surface which enables the synthesis of many generations of protonatable amines. Starburst dendrimers such as PAMAM dendrimers (Figure 1-1B) have been shown to be capable of mediating gene delivery [13]. The surface charge and diameter of the dendrimer are determined by the number of synthetic steps (i.e. number of generations). The number of synthetic steps also determines the particle size after complexation with DNA and transfection efficiency. Unlike PLL, not all the amine groups on PAMAM dendrimers are protonated under physiological conditions.

PEI (Figure 1-1C, D), for the same reason, was considered as a candidate for gene delivery [14]. In fact, PEI is one of the most extensively used cationic polymers to mediate gene delivery. It has the highest cationic charge density in all the organic macromolecule. Every third atom is an amino nitrogen that can be protonated as well as provide a potential branching point. According to its protonation - pH profile [15, 16], approximately 80% of the nitrogens of PEI are not protonated at physiological pH thanks to the containing secondary and tertiary amines. These distinct characteristics give PEI the ability to ionize over a wide pH range. It has been reported that, PEI-based cationic polymers can act as a proton sponge that buffer the decrease in pH, facilitate endosome escape of the PEI/DNA polyplexes, and ultimately increase the efficiency of the sophisticated multistage process of transfection.

There are many novel cationic polymers being developed as potential gene carriers including polysaccharides such as chitosan [17], methacrylate based cationic

polymers [18] and cyclodextrin-containing polymers [19]. Meanwhile polymers based on PLL and PEI are among the most commonly utilized.

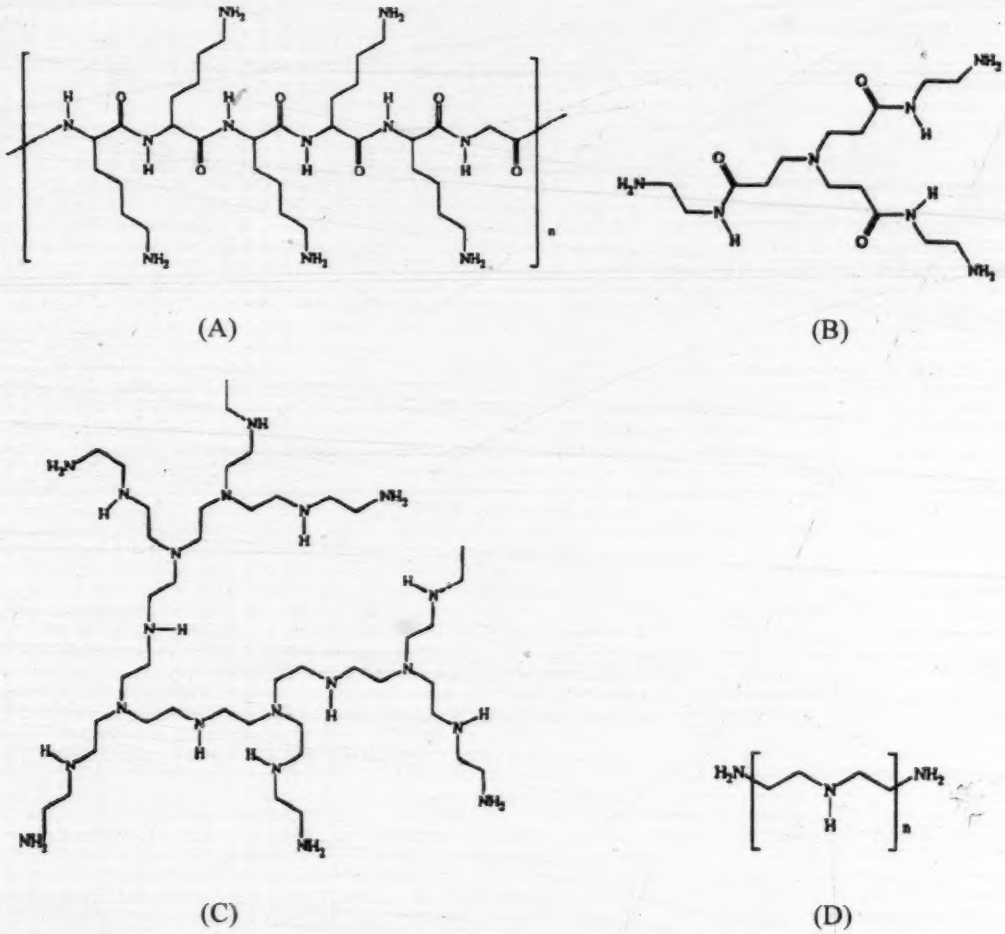

Figure 1-1. The structure of cationic polymers studied as gene carriers: (A) PLL (B) PAMAM dendrimers; (C) Branched PEI; (D) Linear PEI.

1.3 Complex Formation

Effective gene delivery requires that the DNA be delivered to the cells, efficiently internalized by the cell and transported to the nucleolus as schematically shown in Figure 1-2. The condensation of DNA into smaller particles is a crucial step for gene delivery. Upon complexation with cationic polymers, condensed DNA coils occupy only 1/1000-1/10000 of the volume of naked DNA coils [20]. The size and charge density of naked DNA are the two main limitations for them to bind with biological membranes, such as the endothelium, the plasma membrane, and the nuclear membrane. By introducing cationic polymers to the system, negatively charged DNA will be not only neutralized but also condensed. Statistically, coiled cationic polymer collapsed upon mixing with DNA in solution, causing a sharp drop of both the radius and the volume of the supercoiled DNA. Differential scanning calorimetry (DSC) was used to characterize the process and the results showed that cationic polymers were able to destabilize the supercoil structure of DNA permitting potential compaction [21].

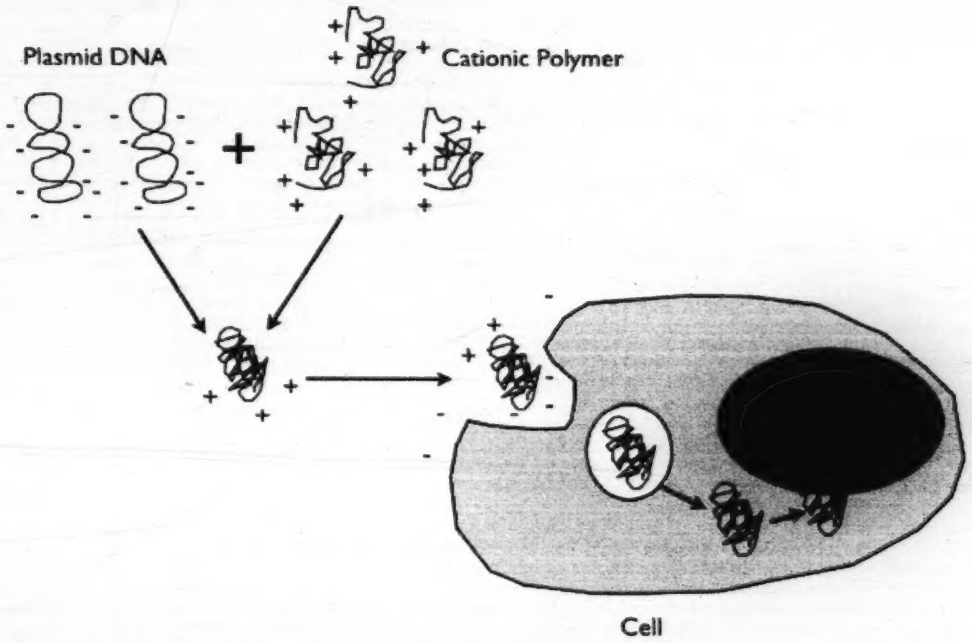

Figure 1-2. Illustration of the non-viral gene delivery multistep process: 1) condensation of DNA into compact particles, 2) uptake into the cells, 3) release from the endosomal compartment into the cytoplasm, 4) uptake of the DNA into the nucleus and finally 5) decondensation of the DNA into a transcribable form.

The interactions of negatively charged DNA with cationic polymers were postulated to be predominantly electrostatic in the process of complex formation. Experiments were conducted allow the exposure of cationic condensing agents such as chitosan and PLL to polyanions (alginate and xanthan) other than DNA. The results did not show any preference of polycations in binding to DNA relative to the competing polyanions [22]. In a separate experiment, DNA was condensed using four cationic polymers with significantly different structures. The morphologies of the unit structures revealed by electron microscope were surprisingly similar [16]. These findings confirmed the hypothesis that the electrostatic interactions, rather than chemical or

structural characteristics, are the determent factor for the condensation and compaction of DNA. Charge neutralization of the polyelectrolytes induces attraction between topologically separated segments and therefore, causes potential condensation. As a matter of fact, from the energetic point of view, the condensation of DNA will spontaneously occur when the charge along the DNA backbone is 90% neutralized [23].

Specific structural properties contribute immensely to the morphology of the polyplexes. Chain stiffness of polymers is believed to set limits on tight curvature, and therefore is one of the most important factors [24]. Theory predicts that semi-flexible macromolecules such as DNA yield stable toroids, while flexible chains should yield amorphous globules upon collapse [25]. This correlates well with the fact that toroidal structures were most commonly observed under electron microscope (EM) [26] and atomic force microscope (AFM) [24] for DNA condensates, independent of the condensing agent used, ranging from small multivalent cations to proteins and polypeptides. In addition, the dimension and morphology of the condensed DNA particles to some extent are surprisingly independent of the size of the DNA. Another factor determining polyplexes morphology is chain length. Spherical globule is reported to be more stable than toroid for long chains [27]. This is in accordance with the findings that condensed by cationic polymers, giant DNA chains with 166 kilo base pair form spherical globules [28]. On the other hand, DNA molecules shorter than 400 base pairs are unable to form orderly, discrete particles upon mixing with cationic condensing agents [29]. Additional to these structural properties, the ionic strength of the solution also influences the morphology of the complexes. It was reported that under high ionic strength, the binding between cationic polymer and DNA was more cooperative

compared to random binding observed at much lower salt concentrations [30]. Proven by Fourier Transform Infrared (FTIR) absorbance spectra, the secondary structure of DNA maintained generally in its B form upon condensation, indicating that there was very little, if any change to the helical form of plasmid DNA [20, 21], though the reduced frequency of the DNA asymmetric phosphate stretching vibrations confirmed DNA's electrostatic interactions with polyamine.

Complexes between PEI and plasmid DNA are typically prepared by simple mixing of polyamine and DNA in an aqueous solution. Electrostatic interactions between the positive charges of the amino groups on polyamine and the phosphate DNA backbones are the main driving force for the polyplex formation. Therefore, the degree of DNA condensation is measured by the N/P ratio. By adopting a more compact structure, DNA is less accessible to small molecules, such as the intercalating dye ethidium bromide, and is protected against degradation by nucleases such as DNase I [31].

1.4 Particle Size

Particle size information obtained from different techniques results in slightly different values. Electron microscopy and light scattering measurements surprisingly revealed that the mean size of the condensed particles did not differ significantly regardless the difference of the molecular weight of the DNA, the sequence of the base pairs and the type of the DNA over a wide range of DNA lengths (400 bp – 50 kbp) [20, 23, 32]. Studies revealed the formation of cationic polymer-DNA complexes with compact toroidal structures of similar size (40 to 60 nm in diameter). The shape and size of the condensed particles were not significantly different among four structurally unique

polymers. However, differences were observed in aggregation behavior. Complexes having less tendency to aggregate demonstrated higher transfection efficiency [21, 33]. Using atomic force microscopy, Dunlap *et al.* showed the completely condensed DNA by PEI to be 20 nm to 40 nm in diameter at N/P ratio equal to 1.6 [34]. While using photon correlation spectroscopy (PCS), PEI-DNA polyplexes hydrodynamic diameters at a different N/P ratio were measured to be 150 nm. These size differences are apparently a result of different ratios used in each study, but it is possible that the difference may be partially due to the use of different techniques or different sample preparation methods.

Several factors can affect particle size of the polymer/DNA complexes. Among them, the most important one is the charge ratio. The charge ratio is defined as the amount of positive charge on the polycations divided by the amount of the negative charge for the DNA. At high positive or negative charge ratios (2 +/- and above), DNA is completely condensed, particles bear same charge. As a result, electrostatic force repels them away from each other. Thus, homogeneous, relatively small particles have been observed. A charge ratio of 1 is stoichiometric point for neutralization. Around this point, since the electrostatic status of the complexes is close to neutral, the repelling force between them is not strong enough to keep them apart. Larger aggregates are formed as a result.

As mentioned, aggregation of complexes is mainly a result of electrostatic interactions. The ionic strength of the solution will therefore affect the particle size. Linear PEI/DNA complexes were reported to form large aggregates at increasing salt concentrations [35], while small complexes prepared under low ionic conditions

remained stable after several days of storage [36]. These findings indicate that charge shielding effect due to higher ionic strength promotes aggregation.

Molecular weight is another factor that influences the particle size of the polymer/DNA complexes. It was observed that complexes formed by low molecular weight PEI with plasmid DNA were significantly larger than those formed by high molecular weight PEI. Moreover, complexes formed with low molecular weight PEI were more likely to aggregate with each other while complexes formed with high molecular weight PEI were relatively stable [21, 37]. The hydrodynamic diameter difference between low molecular weight PEI/DNA complexes and high molecular weight PEI/DNA complexes is mainly because of the reduced DNA condensation of low molecular weight PEI compared with high molecular weight PEI. This led to a weaker compaction of DNA, therefore a larger size.

1.5 Transfection Efficiency

As the interactions between polycations and DNA is mainly electrostatic, cation-to-anion charge ratio immensely affects the transfection efficiency of the polyplexes. It is widely accepted that polyplexes with a slight excess of positive charges have higher transfection efficiency. This probably due to the fact that cell membrane possesses an overall negative charge and the excess positive charge may promote electrostatic interactions between the particles and the anionic cell surface groups, such as proteoglycans. At the same time, the slightly positive charge on the polyplexes may also stabilize the particles and prevent them from aggregation which is a common trend among completely neutralized particles. However, at high N/P ratio where particles bear

high positive charges, the non-specific interactions between the particle and biological fluids, extracellular matrix and non-target cells will be inevitable and adversely affect transfection. The toxicity of the particle will increase substantially, as well.

Another element that influences the overall transfection efficiency is the particle size. In order to pass through the blood circulation, extravasate and diffuse through the tissues, the particle size has to be small enough. Pharmacokinetic studies in vivo indicate that liposomes that exhibit a surface charge and are larger than 200 nm will very likely to be rapidly eliminated from the blood stream. For many applications in vivo, complexes with diameters of 100 nm or less seem to be a necessity to efficiently leave the vascular system and for efficient diffusion through tissue. However, it may not always be the smaller the better. As a matter of fact, for specific applications, slightly larger particle sizes may be more advantageous. Studies done on cationic lipids revealed that relatively large lipoplexes with a diameter ranging from 400 nm to 1400 nm have shown higher transfection efficiency in the cell culture than smaller (smaller than 400 nm) or larger (larger than 1400 nm) ones [36, 38]. Also for branched PEI/DNA complexes, smaller particles have considerably lower transfection efficiency than larger particles both in vitro and in vivo [39, 40]. Those findings imply that the ideal particle size for each specific application might be different depending on the non-viral carrier.

1.6 Zeta Potential

Electrical double layer exists around particles dispersed in a medium. The liquid layer surrounding the particle exists as two regions: an inner part called Stern layer where the counterions are tightly bound to the surface and an outer part known as diffuse layer

where ions are less firmly associated. (See Figure 1-3.) Somewhere within the diffuse layer there is a conceptual boundary inside which the particle acts as a single entity in colloidal system. This boundary is known as the surface of hydrodynamic shear or slipping plane. The potential at this slipping plane is defined as zeta potential. Therefore, zeta potential can be regarded as the effective surface charge of the particle within the dispersed medium.

The magnitude of the zeta potential indicates the potential stability of the colloidal system. If the zeta potential of the particles is high, it means there is a sufficiently high repulsion between the particles so the dispersion will resist flocculation. But if the zeta potential of the particles is close to zero, there is no repulsion mechanism then flocculation or coagulation will eventually take place. The zeta potential is calculated by determining the electrophoretic mobility and then applying the Henry's Equation:

$$U_E = 2 \varepsilon z f(\kappa a) / 3 \eta$$

U_E = electrophoretic mobility
ε = dielectric constant of the sample
z = zeta potential
$f(\kappa a)$ = Henrys function, where κa is the ratio of particle radius to double layer thickness. For particles in polar media, $f(\kappa a) = 1.5$ (Smoluchowski approximation)
η = viscosity of the solvent

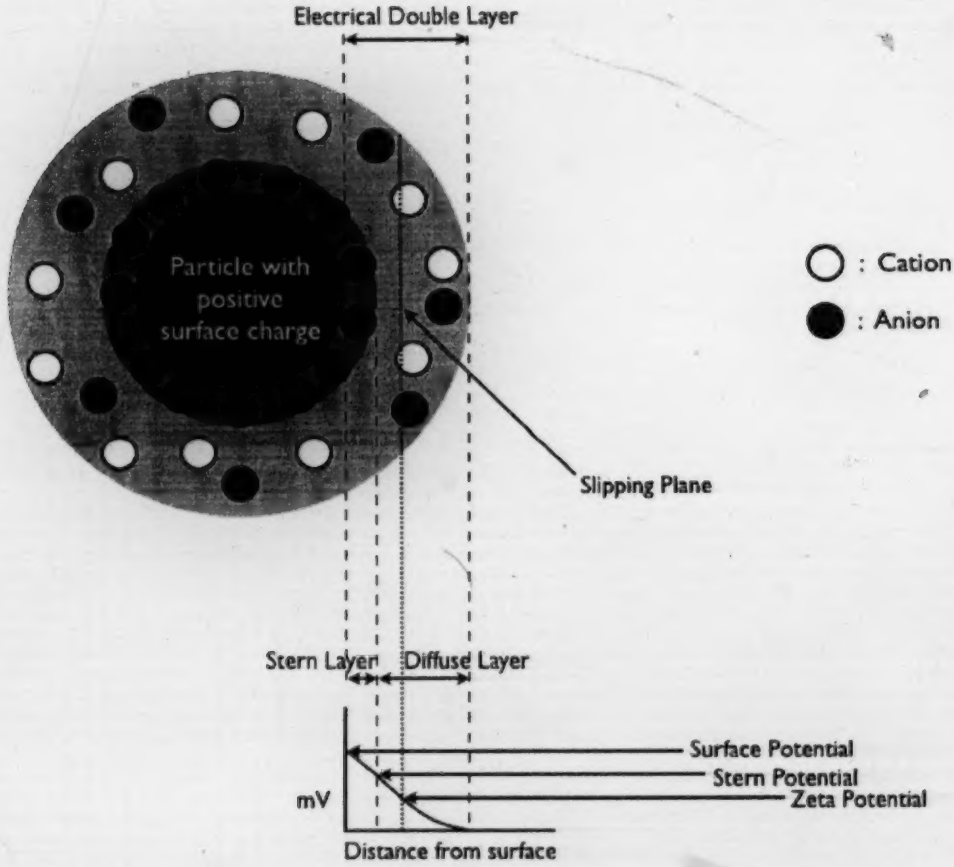

Figure 1-3. Illustration of the concept of Stern layer, diffuse layer, slipping plane and zeta potential.

Although the average zeta potential value is usually the basis of most studies available in literature [37, 41, 42], sometimes analyses of data using the average zeta potential of the particles alone will neglect the detail information about the attachment behavior caused by the variation of particle zeta potentials. This can potentially lead to misleading and counterfactual conclusions. The detailed zeta potential distribution provides a good way to study the heterocoagulation phenomena in aqueous media for a two-component system. [43]

1.7 Photon Correlation Spectroscopy (PCS)

PCS is based on theory of light scattering. It is also called Dynamic Light Scattering (DLS). When a beam of light passes through a colloidal dispersion, the particles or droplets scatter some of the light in all directions. For particles smaller than a tenth of the wavelength of the light, scattering is equal in all directions. Rayleigh theory postulates that the intensity of the scattered light is directly proportional to the diameter of the particle to the sixth power. When the size of the particles become equivalent to the wavelength of the laser, the scattering changes from being isotropic to a distortion in the forward scattering direction and becomes a complex function showing maxima and minima with respect to angle. A theory developed by Mie explained the phenomena and allowed transformation of the measured intensity distribution data to volume. This theory is used in Zetasizer 3000 HSA for particle size determination.

Briefly, in order to get the particle size information from dynamic light scattering methods, Brownian motion are measured, diffusion rate are obtained and then particle sizes are calculated. Brownian motion is the random movement of particles in a fluid due to the bombardment by the solvent molecules that surround them. Brownian motion is inversely proportional to particle size, i.e. a large particle will diffuse slower than a small particle. The velocity of the Brownian motion is defined by the translational diffusion coefficient (D). Once the translational diffusion coefficient is measured, the hydrodynamic diameter of the particle will be calculated by using the Stokes-Einstein Equation:

$$d(H) = k T / 3 \pi \eta D$$

d(H)	=	hydrodynamic diameter
k	=	Boltzmann's constant
T	=	absolute temperature
η	=	viscosity of the medium
D	=	translational diffusion coefficient

The diameter measured by dynamic light scattering is a value that refers to how a particle moves within the medium. Therefore, it is called the hydrodynamic diameter, which means the diameter obtained is the diameter of a sphere that has the same translational diffusion coefficient as the actual particle. The hydrodynamic diameter is somewhat different from the real size of the particle. Actually, it is the sum of the particle size and the thickness of the electrical double layer (Debye length). The thickness of the electrical double layer is dependent on the ionic strength of the medium. Under low ionic strength condition, the double layer is extended, while in high ionic strength media, the double layer is suppressed. The geometry of non-spherical particles might influence the uniformity of their diffusion coefficient, but the hydrodynamic diameter reported would be based upon the sphere that has the same average diffusion coefficient as that of the particles.

1.8 Atomic Force Microscopy (AFM)

Information about the size of the particles is crucial in gene delivery applications [20, 23, 32, 44]. AFM as a relatively new technique is complementary to PCS method in determining particle size. AFM, also known as Scanning Probe Microscopy (SPM) is a high-resolution imaging technique developed in 1986 [45]. It provides three-dimensional surface topography at nanometer lateral and subangstrom vertical resolution. AFM

works by scanning a sharp tip on the end of a cantilever across the sample surface while maintaining a small, constant force between the tip and the sample surface. The ionic repulsive force between the surface and the tip bends the cantilever upwards. The amount of bending is measured by deflection of reflecting laser beam off the back of the cantilever into a split photodiode detector. By detecting the difference in the photodetector output voltages, changes in the cantilever deflection or displacement amplitude are determined to keep the force constant while scanning the tip across the surface. The vertical movement of the tip follows the surface profile and is recorded as the surface topography by the AFM. Schematics of how AFM works is illustrated in Figure 1-4.

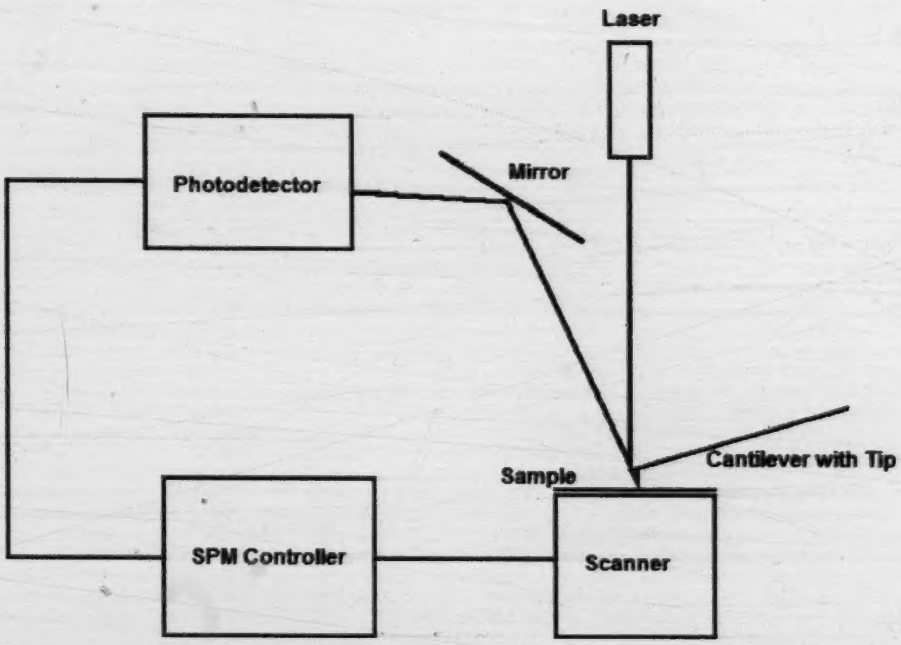

Figure 1-4. An illustration of the AFM operation. A laser beam is pointed to the tip of the cantilever and reflected to the photodetector. Bending of the cantilever is then detected and the scanner is vertically adjusted to keep the force between the tip and sample constant. By recording the movement of the scanner, the three dimensional topology of the sample surface is generated.

AFM provides a number of advantages over conventional microscopy techniques. Unlike its predecessor, Scanning Tunneling Microscope (STM) which requires the samples to be conductive, AFM is applied to both conductors and insulators. Furthermore, AFM offers the advantage that the writing voltage and tip-to-substrate spacing can be controlled independently, whereas with STM the two parameters are integrally linked. Different from Scanning Electron Microscope (SEM) which usually requires samples to be coated prior to the experiment, AFM provides exceptional topographic contrast, direct height measurements and unobscured views of surface features. Compared with Transmission Electron Microscopes (TEM), sample preparation of AFM is much easier and less expensive. At the same time, the three dimensional information revealed by AFM is far more complete than morphology obtained by TEM. Last but not least, AFM not only has unequivocal resolution advantage over optical microscopy, it also provides explicit measurement of step heights, regardless the reflectivity differences between materials. Table 1-1 summarized the comparison of AFM with other microscopy techniques.

Table 1-1. Comparison of AFM with other microscopy techniques: TEM, SEM and optical microscopy.

	AFM	TEM	SEM	Optical
Max resolution	Atomic	Atomic	1 nm	0.1 μm
Imaging Environment	air, fluid, vacuum, special gas	vacuum	vacuum	air, fluid
In-situ	Yes	No	No	Yes
In fluid	Yes	No	No	Yes
Sample preparation	Easy	Difficult	Easy	Easy

There are mainly two basic types of AFM scanning techniques: contact mode and tapping mode. In contact mode, the cantilever with tip scans the sample in close contact with the surface. The deflection of the cantilever is sensed and compared to a preset value of deflection and the distance between the sample and the cantilever is then adjusted by raising or lowering the sample in order to restore the desired value of deflection. The force on the tip is a repulsive force with a mean value of 10^{-9} N and is set by pushing the cantilever against the sample surface with a piezoelectric positioning element. This could potentially cause damage or alteration to samples that are soft, fragile, or loosely attached to the substrate. Tapping mode overcomes these problems by introducing a tip that is oscillating at or near its resonance frequency. The vertically oscillating tip alternately contacts the surface to provide high resolution and lifts off the surface to avoid dragging the tip across the surface. This approach virtually eliminates the lateral, shear forces present in contact mode that can damage the samples. Tapping mode AFM is therefore successfully used for biological samples.

2. SCOPE

The primary objectives of this thesis include the study of the interactions between DNA and PEI, the attempt to predict and control DNA/PEI complexes by changing different parameters, and the kinetic study of DNA/PEI complexes formation. We characterized the biophysical properties of the condensed DNA complexes by cationic polymer (PEI), specifically the zeta potential and size of particles. Those properties are well documented to be crucial in the transfection performance of such system in vivo.

Zeta potential of the complexes in different mediums was measured and analyzed. In this study, linear DNA was used as substitute of plasmid DNA as they shared the same four bases (adenine, thymine, cytosine and guanine). The plasmid and linear DNA were of similar charge density. Zeta potential distribution analysis helped us understand the actual charging status of the particles within the solution. Particle size was also measured by Photon Correlation Spectroscopy, and correlation between zeta potential and particle size was studied. The other aim of this study was to find a way to control the zeta potential and particle size of the DNA-cationic polymer complexes. Therefore, we changed ionic strength and pH values of the media to perform these measurements.

By utilizing AFM, we generated the actual three-dimensional topography of the complex surface and measured the actual particle size of the DNA-cationic polymer complexes instead of the hydrodynamic diameter. AFM also provided us the tool to further investigate the interactions between plasmid DNA and cationic polymer by taking AFM images at different incubation time. This set of experiment helped us explore the

condensation mechanism and provided insights on how to control the particle size of the complexes.

In summary, this study generated us useful information about the charge and size of the DNA-cationic polymer complexes. For the first time, kinetic study of DNA/PEI complex formation was investigated, and zeta potential distribution was used to explore the heterocoagulation phenomena in the DNA/PEI solution. It also provided a practical guidance to control those properties. Combined with transfection efficiency studies, it will give us new insights on designing better gene delivery systems and smart tools to evaluate them.

3. MATERIALS AND METHODS

3.1 Materials

Polyethylenimine (PEI, Mw~25,000 Da) and Poly (acrylic acid) (PAA, Mw~750,000 Da) were purchased from Aldrich (Milwaukee, WI). Polymers were diluted in H_2O and dialyzed against deionized H_2O for 72 hours prior to their use. Sodium phosphate monobasic, mono hydrate ($NaH_2PO_4 \cdot H_2O$, 137.99 g/mol), sodium phosphate dibasic, anhydrous (Na_2HPO_4, 141.96 g/mol) and sodium chloride (NaCl, 58.44 g/mol) were obtained from EMD Chemicals. Phosphate buffer was prepared by mixing an appropriate volume of (**A**) 100 mM sodium phosphate monobasic, mono hydrate (13.8 g/L) and (**B**) sodium phosphate dibasic, anhydrous (14.2 g/L) to give certain pH values. Molecular porous membrane tubing for dialysis was manufactured by Spectrum Laboratories (Rancho Dominguez, CA).

Linear DNA from salmon sperm (2 kbp, 20μL per aliquot, concentration 9.9 mg/mL) was purchased from Sigma Aldrich Corp. Plasmid DNA (pEGFP, 4.7 kbp) containing a red-shifted variant of wild-type green fluorescent protein (GFP) and a kanamycin resistance gene was replicated in the kanamycin resistant DH5-α *E. coli* strain grown in Luria-Bertani medium. The plasmid DNA was purified using Plasmid Giga Kit from QIAgen and the purified plasmid was diluted to 0.4 mg/mL in TE buffer (10 mM Tris-Cl, 1mM EDTA at pH 8.0). The purity and concentration of the plasmid DNA were confirmed by UV spectroscopy.

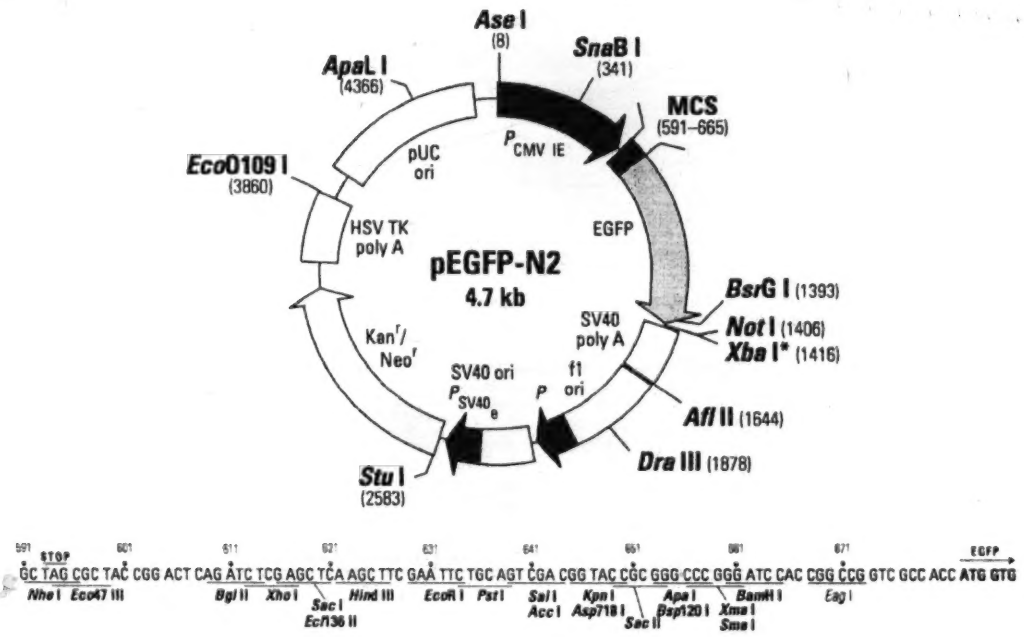

Figure 2-1. The restriction map and multiple cloning site of pEGFP-N2.

In order to prepare 1 L of 100 mM phosphate buffer at given pH (pH=5.0, 6.0, 7.0 and 8.0), 900 mL of distilled water was combined with the appropriate amounts of $NaH_2PO_4 \cdot H_2O$ and Na_2HPO_4 stock solutions calculated to obtain the desired pH. The pH values were checked and adjusted when necessary. Then more distilled water was added to bring the total volume to 1 L. The final pH values were then checked again. To prepare NaCl buffer, the calculated amount of NaCl was weighed and transferred to a container. Distilled water or other solutions were added to bring the final concentration to the desired value.

3.2 Analysis by Zetasizer

Zetasizer 3000 HSA was manufactured by Malvern Instruments Ltd., Worcestershire, UK. It is a particle size and zeta potential analyzer. The size range it can measure is from 2 nm to 3 microns. For electrophoresis, the applicable size range is from 10 nm to 30 μm.

3.2.1 Zeta Potential Analysis

Polymers were dissolved in deionized water and dialyzed against water for three days. Deionized water (~ 0 mV) and clay suspension (~ -20 mV) samples were measured by Zetasizer and checked to ensure the accuracy of the instrument before each set of measurements.

3.2.1.1 Complex Formation

3.2.1.1.1 PEI/PAA Complexes

PEI and PAA were dissolved in deionized water separately and dialyzed against H_2O for three days before experiment. Concentrations were confirmed after dialysis. Specific amount of PEI and PAA solutions were added into the tube for each sample, then deionized water was added to dilute it to desired concentrations. Samples were votexed vigorously for 20 seconds and incubated for 20 minutes at room temperature for complex formation. Zeta potential was then measured using a Malvern Zetasizer 3000 HSA. Solutions containing PEI or PAA only were also measured as controls. Table 2-1 listed the concentration of PEI and PAA for each sample in zeta potential measurements.

Table 2-1. The concentration of PEI and PAA used for PEI/PAA complex zeta potential measurements.

PEI Conc. (μg/mL)	PAA Conc. (μg/mL)	PEI/PAA Mass Ratio
10	30	0.33
10	20	0.5
10	10	1
10	5	2
10	3.3	3
5	15	0.33
5	10	0.5
5	5	1
5	2.5	2
5	1.67	3
1	3	0.33
1	2	0.5
1	1	1
1	0.5	2
1	3.3	3
5	0	N/A
0	5	N/A
1	0	N/A
0	1	N/A

3.2.1.1.2 PEI/Linear DNA

Different amount of PEI and linear DNA solutions were mixed in the tube for each sample. Samples were diluted by specific solutions (deionized water, sodium chloride buffer or phosphate buffer at certain pH value) until final DNA concentration reached 10 μg/mL. Then samples were votexed vigorously for 20 seconds and incubated at room temperature for 20 minutes to allow complex formation before zeta potential measurement.

In order to study how size/zeta potential change as function of PEI/DNA ratio, different mass ratio of PEI/DNA (2:1, 1:1, 2:1, 4:1, 8:1 and 12:1) were mixed. NaCl buffer (30 mM and 150 mM) were introduced to investigate the effect of ionic strength to

the zeta potential/size of the complexes in the solution. To see the effect of pH on size/zeta potential, phosphate buffers were introduced at pH=5.0, 6.0, 7.0 and 8.0. At a given pH, ionic strength was also changed by adding NaCl (30 mM and 150 mM) into the solution. Table 2-2 shows the concentration of PEI and DNA for each sample in zeta potential measurements.

Table 2-2A. The concentration of PEI and DNA used for PEI/DNA complex zeta potential measurements in H_2O.

PEI Conc. (μg/mL)	DNA Conc. (μg/mL)	PEI/DNA Mass Ratio
5	50	0.1
5	25	0.2
5	20	0.25
5	15	0.33
5	10	0.5
5	5	1
5	2.5	2
5	1.67	3

Table 2-2B. The concentration of PEI and DNA used for PEI/DNA complex zeta potential measurements in NaCl buffers (30mM and 150 mM).

NaCl Conc. (mM)	PEI Conc. (μg/mL)	DNA Conc. (μg/mL)	PEI/DNA Mass Ratio
30	1.875	15	0.125
	2.5	10	0.25
	5	10	0.5
	10	10	1
	20	10	2
150	2.5	10	0.25
	5	10	0.5
	5	5	1
	20	10	2

Table 2-2C. The concentration of PEI and DNA used for PEI/DNA complex zeta potential measurements in phosphate buffer at different pH with NaCl concentration of 30 mM.

pH	PEI Conc. (μg/mL)	DNA Conc. (μg/mL)	PEI/DNA Mass Ratio
5.0	2.5	20	0.125
	2.5	10	0.25
	5	10	0.5
	10	10	1
	20	10	2
6.0	2.5	20	0.125
	2.5	10	0.25
	5	10	0.5
	10	10	1
	20	10	2
7.0	2.5	20	0.125
	2.5	10	0.25
	5	10	0.5
	5	6.7	0.75
	10	10	1
	20	10	2
8.0	5	10	0.5
	10	10	1
	20	10	2

Table 2-2D. The concentration of PEI and DNA used for PEI/DNA complex zeta potential measurements in phosphate buffer at different pH with NaCl concentration of 150 mM.

pH	PEI Conc. (μg/mL)	DNA Conc. (μg/mL)	PEI/DNA Mass Ratio
5.0	1.875	15	0.125
	2.5	10	0.25
	5	10	0.5
	10	10	1
	20	10	2
6.0	2.5	10	0.25
	5	6.7	0.5
	5	10	0.75
	10	10	1
	20	10	2

3.2.1.2 Zeta Potential Measurement

Zeta potential measurements were carried out with a Malvern Zetasizer 3000 HSA, which was equipped with a standard capillary electrophoresis cell. The capillary cell in which the samples were loaded was washed by deionized water several times and left in an ultrasonic bath (Fisher) for about 30 min before zeta potential measurements. After the Zetasizer was powered on each time, temperature was set to 25°C. The first sample was loaded after no less than 15 minutes for the instrument to warm up. About 5 ml of the sample was transferred to the capillary cell via a single use syringe. Zeta potential measurement was performed 10 minutes after sample loading, for the temperature to stabilize at 25±0.1°C. The sampling time was set to automatic. Average values were calculated with data from five consecutive runs. There were 20-second intervals between each runs as well as before the first run. The capillary cell was thoroughly flushed by approximately 20 ml deionized water before loading the next sample.

Using Zetasizer 3000 HSA, electrophoretic mobility was measured and zeta potential was then calculated by the zeta potential measurement program using the Henry's Equation.

3.2.2 Zeta Potential Distribution Analysis

For each sample, three zeta potential distribution diagrams were overlapped and analyzed using the Zetasizer software.

3.2.3 Photon Correlation Spectroscopy (PCS)

The hydrodynamic diameters of the complexes were measured by PCS using Zetasizer 3000 HSA. Samples were prepared as described earlier and transferred to the disposable polystyrene cuvettes. Scattered light was detected at a 90° angle through a 400 μm pin hole at 25°C. PCS size measurements for each sample were performed three times and the values were averaged. For temperature to be stable at 25°C, there was a 10 minutes interval between sample loading and the first measurement. For the data analysis, the viscosity (0.8905 mPa•s) and refractive index (1.333) of pure water at 25°C were used. Table 2-3 lists the concentration of PEI and PAA for each sample in particle size measurements. Table 2-4 and Table 2-2D show the concentration of PEI and DNA used for PEI/DNA complex particle size measurements in different media.

Table 2-3. The concentration of PEI and PAA used for PEI/PAA complex particle size measurements.

PEI Conc. (μg/mL)	PAA Conc. (μg/mL)	PEI/PAA Mass Ratio
10	30	0.33
10	20	0.5
10	10	1
10	5	2
10	3.3	3

Table 2-4A. The concentration of PEI and DNA used for PEI/DNA complex particle size measurements in H_2O.

PEI Conc. (μg/mL)	DNA Conc. (μg/mL)	PEI/DNA Mass Ratio
5	50	0.1
5	25	0.2
5	20	0.25
5	10	0.5
5	5	1
0.5	5	0.1
0.625	5	0.125
0.83	5	0.167
1.25	5	0.25
1.67	5	0.33
5	5	1

Table 2-4B. The concentration of PEI and DNA used for PEI/DNA complex particle size measurements in NaCl buffers (30 mM and 150 mM).

NaCl Conc. (mM)	PEI Conc. (μg/mL)	DNA Conc. (μg/mL)	PEI/DNA Mass Ratio
30	1.875	15	0.125
	2.5	10	0.25
	5	10	0.5
	10	10	1
	20	10	2
150	1.875	15	0.125
	2.5	10	0.25
	5	10	0.5
	10	10	1
	20	10	2

Table 2-4C. The concentration of PEI and DNA used for PEI/DNA complex particle size measurements in phosphate buffer at different pH with NaCl concentration of 30 mM.

pH	PEI Conc. (μg/mL)	DNA Conc. (μg/mL)	PEI/DNA Mass Ratio
5.0	2.5	20	0.125
	2.5	10	0.25
	5	10	0.5
	10	10	1
	20	10	2
6.0	2.5	20	0.125
	2.5	10	0.25
	5	10	0.5
	10	10	1
	20	10	2
7.0	2.5	20	0.125
	2.5	10	0.25
	5	10	0.5
	5	6.7	0.75
	10	10	1
	20	10	2
8.0	2.5	20	0.125
	2.5	10	0.25
	5	10	0.5
	10	10	1
	20	10	2

3.3 Analysis by Atomic Force Microscope

The MultiMode SPM (Digital Instruments Inc., Santa Barbara, CA) was used for all AFM imaging. It is designed for imaging small (approx. 1.5 cm diameter) samples using a series of interchangeable scanners and is able to provide images from the atomic scale to 175 μm in size. A large-area scanner (J type) with a maximum *xy* scan range of 125 μm × 125 μm and a *z* vertical range of 5 μm was used most of the time except for imaging naked plasmid DNA, in which case a small-area scanner (A type) with a maximum *xy* scan range of 0.4 μm × 0.4 μm and a *z* vertical range of 0.4 μm was used for higher resolution. Single crystal silicon cantilevers (Digital Instruments Inc.) were cleaned by exposure to high intensity UV light for 3 minutes before use. All AFM imaging was conventional ambient tapping mode AFM. The amplitude of the scanning tip tapping registered 0.5 V and the frequency of the tapping was in the range of 200-400 kHz. The scan rate was typically 1.0-2.0 Hz. The data collection was set at 512 × 512 pixels. Images were processed and analyzed using the Nanoscope III software version 5.12.

3.3.1 Imaging of PEI/Linear DNA Complexes Under AFM

The PEI/linear DNA solutions with different mass ratio in water were prepared. DNA concentrations were 30 μg/mL and 10 μg/mL. After 30 minutes incubation at room temperature, 1.5 μL DNA/PEI aqueous solutions were loaded onto the center of a freshly cleaved untreated mica disk. After adsorption for 5 minutes at room temperature, excess solution was removed by soaking into filter paper and the mica surface was further dried at room temperature for 30 minutes before imaging with AFM operating in tapping mode.

Particle areas were measured for those whose heights exceeded a user-defined threshold. Equivalent diameters for the particles were calculated assuming a circular geometry.

3.3.2 Imaging Naked Plasmid DNA Under AFM

Plasmid DNA solution of 0.4 mg/mL was prepared as mentioned earlier. It was further diluted to 5 μg/mL with water and 2.5 μg/mL with 3 mM NaCl buffer, respectively, then votexed for 10 seconds to ensure well mixing. A 10 μL of this solution was transferred onto freshly cleaved mica. After 3 minutes adsorption, the mica disk was dipped into water. The excess water was removed by filter paper. After drying at room temperature for 30 minutes, the surface was blow-dried thoroughly by nitrogen when necessary. The samples were then imaged with AFM operating in tapping mode. A small-area scanner (A type) was used for higher resolution. Section analysis was performed using the Nanoscope III software.

3.3.3 Investigation of Complex Formation Under AFM

Plasmid DNA and PEI were dissolved separately in 3mM NaCl solution. Calculated amount of plasmid DNA and PEI solutions were transferred to a tube maintaining PEI/DNA mass ratio of 1 and the final DNA concentration of 2.5 μg/mL. The solution was well mixed by vortexing for 10 seconds. At each time points (1 min, 10 min, 30 min), 10 μL of this solution was transferred onto freshly cleaved mica. After 3 minutes adsorption, the mica disk was dipped into water. The excess water was removed by filter paper. After further drying it for 5 minutes, surface was blow-dried thoroughly by nitrogen. The samples were then imaged with AFM operating in tapping mode.

3.3.4 Imaging of PEI/Plasmid DNA Complexes With AFM

The PEI/linear DNA solutions of different mass ratio in water were prepared. DNA concentrations were 2.5 μg/mL. After 30-minute incubation at room temperature, 1.5 μL DNA/PEI aqueous solutions were loaded onto the center of a freshly cleaved mica disk. After adsorption for 5 minutes at room temperature, excess solution was removed by soaking into filter paper and the mica surface was further dried at room temperature for 30 minutes before imaging. Then sample was imaged with AFM operating in tapping mode. Particle areas were measured for those whose heights exceeded a user-defined threshold. Those whose diameter was less than 25 nm were ignored as they were unlikely to contain entire plasmids. Equivalent diameters for the particles were calculated assuming a circular geometry.

4. RESULTS

4.1 Zeta Potential Analysis

4.1.1 PEI/PAA Complexes in H_2O

Anionic polymer PAA was initially used as a substitute for negatively charged DNA. The reason for this was that DNA was not readily available in large quantities so that initial studies to test the instrument were performed with relatively inexpensive PAA. Combined with cationic PEI, the negatively charged PAA was expected to form complexes in buffer solution. The zeta potential of those complexes was measured by the Zetasizer.

The results of the zeta potential measurements of PEI/PAA complexes are summarized in Table 3-1. There were three different series of samples, differing in the final concentration of PEI in samples, a) PEI = 10 μg/mL, b) PEI = 5 μg/mL, c) PEI = 1 μg/mL. Within each series, PAA concentration was varied and PEI/PAA mass ratio was maintained at 0.33, 0.5, 1, 2 and 3. There were also controls with PEI only (PAA = 0 μg/mL) and PAA only (PEI = 0 μg/mL) for concentration at 5 μg/mL and 1 μg/mL of PEI and PAA, respectively.

Figure 3-1 shows that the zeta potential of the complexes changes as a function of PEI/PAA mass ratio. Three main features were evident from this figure: 1) For all three series of samples, the zeta potential always increased as the PAA concentration decreased (i.e. PEI/PAA mass ratio increased). 2) For samples with PEI concentration at both 10 μg/mL and 5 μg/mL, standard deviations in zeta potential were small, i.e. the results were reproducible. For samples with PEI concentration at 1 μg/mL, standard deviations in zeta

potential were relatively larger, but the results were still quite reproducible both at high end and low PEI/PAA mass ratio. 3) The zeta potential of the complexes was independent of the PEI concentration at 10 and 5 μg/mL. At 1 μg/mL, the zeta potential was in similar range with the other two series for high PAA concentration samples, but at low PAA concentration, the maximum zeta potential was 29.6 mV compared to 48.0 mV and 46.3 mV for PEI concentration of 10 μg/mL and 5 μg/mL.

Table 3-1. The characteristic of PEI/PAA samples used for zeta potential measurements and average zeta potential values of the PEI/PAA complexes.

PEI Conc. (μg/mL)	PAA Conc. (μg/mL)	PEI/PAA Mass Ratio	Mean Zeta Potential (mV)	SD (mV)	CV
10	30	0.33	-19.6	0.2	1.02%
10	20	0.5	-12.6	2.2	17.5%
10	10	1	29.8	0.8	2.7%
10	5	2	48.0	0.8	1.7%
10	3.3	3	47.4	0.8	1.7%
5	15	0.33	-20.8	0.3	1.4%
5	10	0.5	-7.7	0.6	7.8%
5	5	1	19.4	1.5	7.7%
5	2.5	2	46.3	1.4	3.0%
5	1.67	3	46.3	1.5	3.2%
1	3	0.33	-18.7	0.9	4.8%
1	2	0.5	1.8	1.2	66.7%
1	1	1	19.0	7.0	36.8%
1	0.5	2	29.6	3.0	10.1%
1	3.3	3	23.0	2.0	8.7%
5	0	N/A	5.6	1.4	25.0%
0	5	N/A	-1.0	1.2	120.0%
1	0	N/A	5.5	4.7	85.4%
0	1	N/A	-2.5	8.4	336.0%

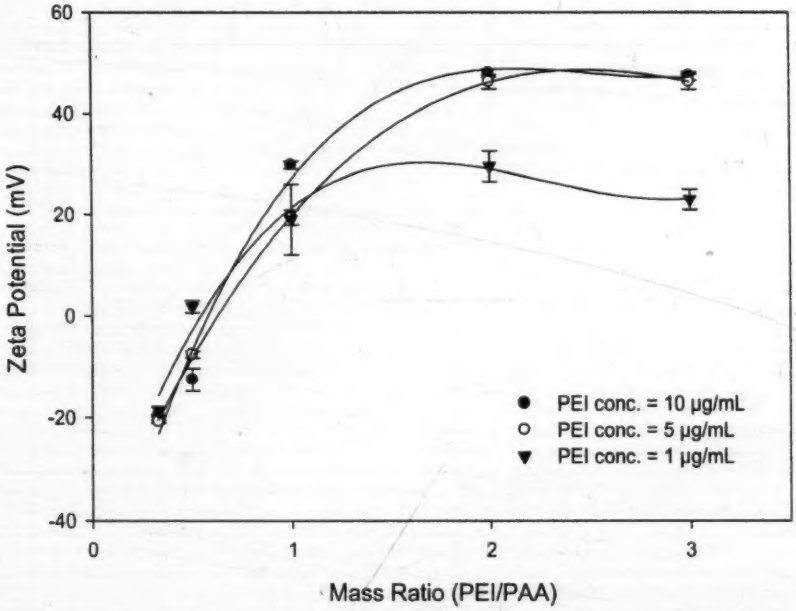

Figure 3-1. The average zeta potential of PEI/PAA complexes as a function of PEI/PAA mass ratio. The results are shown as mean values (± SD) of 3 measurements. Where no standard deviation is visible, they are smaller than the symbols used.

4.1.2 PEI/Linear DNA Complexes in H_2O

Since the results from last series of experiments were relatively reproducible, and for PEI concentration between 5 µg/mL and 10 µg/mL, the zeta potential values were very similar to each other, we next tested PEI complexation with linear DNA. Linear DNA from salmon sperm was used because it contains the same four bases (adenine, thymine, cytosine and guanine), therefore has the same chemical nature and the negative charge per weight as a plasmid DNA. PEI concentration was chosen as 5 µg/mL for all the samples in this set of experiments. DNA concentrations were altered to make PEI to DNA mass ratio vary from 0.1 to 3. The sample properties used for this study and the results of this study are summarized in Table 3-2.

Table 3-2. The characteristic of PEI/linear DNA samples used for zeta potential measurements and average zeta potential values of the PEI/linear DNA complexes.

PEI Conc. (μg/mL)	DNA Conc. (μg/mL)	PEI/DNA Mass Ratio	Mean Zeta Potential (mV)	SD (mV)	CV
5	50	0.1	-20.5	4.8	23.4%
5	25	0.2	-19.8	2.2	11.1%
5	20	0.25	-6.8	1.3	19.2%
5	15	0.33	30.2	0.3	1.0%
5	10	0.5	44.8	1.2	2.7%
5	5	1	40.8	5.5	13.5%
5	2.5	2	33.6	4.4	13.1%
5	1.67	3	46.8	6.5	13.9%

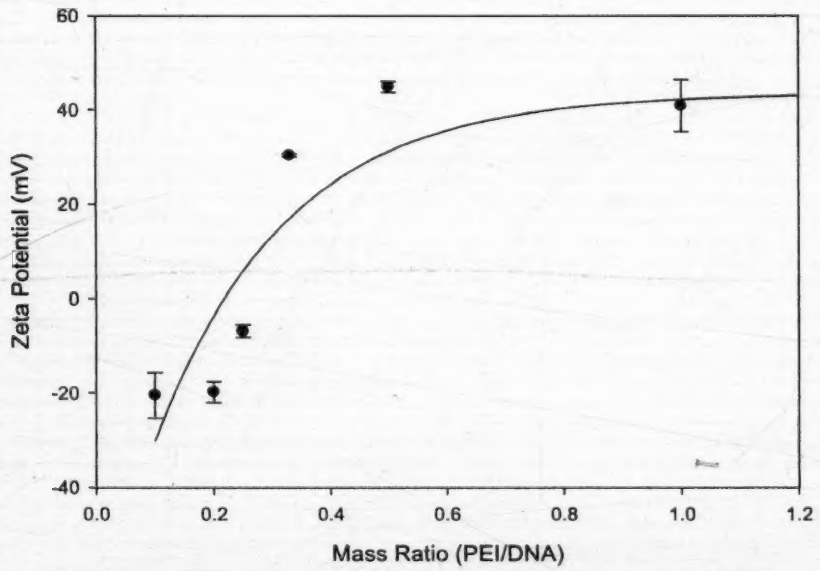

Figure 3-2. The average zeta potential of PEI/linear DNA complexes in H_2O as a function of PEI/linear DNA mass ratio. The results are shown as mean values (± SD) of 3 measurements. Where no standard deviation is visible, they are smaller than the symbols used.

Figure 3-2 shows the change of zeta potential of the PEI/linear DNA complexes as a function of PEI/linear DNA mass ratio. Three main results were evident from this

figure: 1) The zeta potential was strongly negative for low PEI/DNA mass ratio, and as the mass ratio increased from 0.1 to 0.5, the zeta potential increased as DNA concentration decreased (i.e. PEI/linear DNA mass ratio increased). At high PEI/linear DNA mass ratio from 0.5 to 3, the zeta potential of the complexes was strongly positive, varying between 33.6 to 46.8 mV with no significant change in this range. 2) At PEI/linear DNA mass ratio around 0.25, the zeta potential of the PEI/linear DNA complexes was close to neutral. 3) For PEI/linear DNA mass ratio at 0.2, 0.25, 0.33 and 0.5, standard deviations were small, i.e. the results were relatively reproducible in this range.

4.1.3 PEI/Linear DNA Complexes in NaCl Solution

Solution conditions (ionic strength and pH) were then changed and controlled to study their effects on zeta potential of the particles. NaCl was introduced to the solution in order to set the ionic strength of the solution to 30 and 150 mM. PEI/linear DNA mass ratio for each series of experiments were maintained to be 0.12, 0.25, 0.5, 1 and 2, while the PEI and DNA concentrations were varied when it was necessary to keep the Zetasizer's count rate in the optimal range. The results of this study are summarized in Table 3-3.

Figure 3-3 shows how the zeta potential of PEI/linear DNA complexes in 30 and 150 mM NaCl solution changes with PEI/linear DNA mass ratio. For PEI/linear DNA mass ratio at 0.25 to 1.00, the zeta potential increases as DNA concentration decreases. At higher PEI/linear DNA mass ratio (0.50, 1.00 and 2.00), the zeta potential of

PEI/linear DNA complexes in 30 mM NaCl buffer kept increasing gradually to 23.9 mV while in 150 mM NaCl buffer, it dropped to 9 mV after peaked at around 30 mV.

Table 3-3. The characteristic of PEI/linear DNA samples used for zeta potential measurements and average zeta potential values of the PEI/linear DNA complexes in NaCl.

NaCl Conc. (mM)	PEI Conc. (µg/mL)	DNA Conc. (µg/mL)	PEI/DNA Mass Ratio	Mean Zeta Potential (mV)	SD (mV)	CV
30	1.875	15	0.125	-20.8	8.3	39.9%
	2.5	10	0.25	-27.7	4.1	14.8%
	5	10	0.5	9.0	1.6	17.8%
	10	10	1	16.1	5.1	31.7%
	20	10	2	23.9	2.6	10.9%
150	2.5	10	0.25	-29.8	0.8	2.7%
	5	10	0.5	19.4	1.6	8.2%
	5	5	1	28.9	2.2	7.6%
	20	10	2	9.4	3.4	36.2%

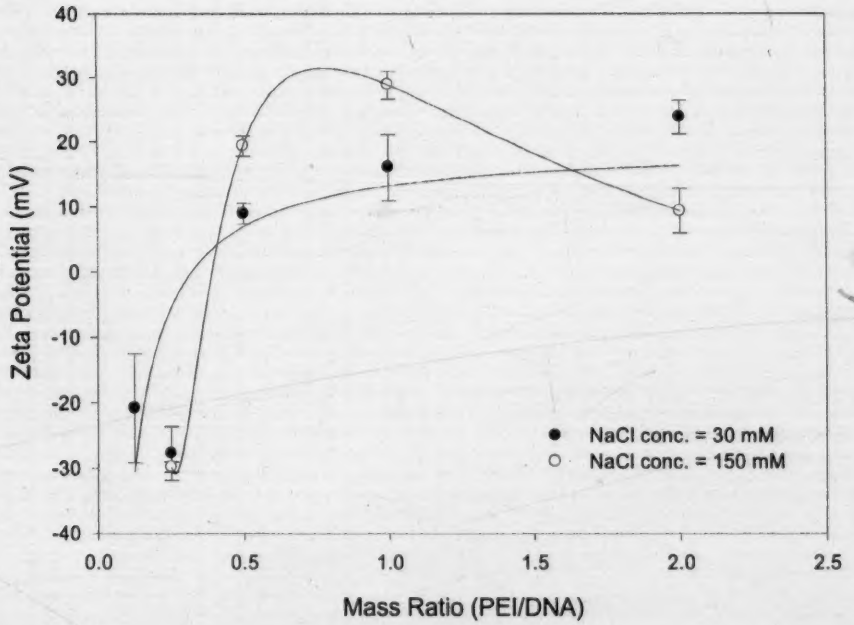

Figure 3-3. The average zeta potential of PEI/linear DNA complexes in NaCl buffers (30 mM and 150 mM) as a function of PEI/linear DNA mass ratio. The results are shown as mean values (± SD) of 3 measurements.

4.1.4 PEI/Linear DNA Complexes in Phosphate Buffer

In order to investigate the effect of pH on solution's electrophoresis, phosphate buffers at different pH (5.0, 6.0, 7.0 and 8.0) were utilized to control the pH value of the solution. Meanwhile, NaCl concentrations were controlled at 30 and 150 mM in the two series of samples. Table 3-4A summarizes the results of the zeta potential measurements in 30 mM NaCl solutions at different pH. As previously stated, PEI/DNA mass ratios

were controlled, but specific concentrations were changed in order to get optimal count rate from the Zetasizer.

Table 3-4A. The characteristic of PEI/linear DNA samples used for zeta potential measurements and average zeta potential values of the PEI/linear DNA complexes in phosphate buffer (NaCl conc. =30 mM).

pH	PEI Conc. (μg/mL)	DNA Conc. (μg/mL)	PEI/DNA Mass Ratio	Mean Zeta Potential (mV)	SD (mV)	CV
5.0	2.5	20	0.125	-36.1	1.9	5.3%
	2.5	10	0.25	-33.8	2.7	8.0%
	5	10	0.5	-9.3	1.1	11.8%
	10	10	1	8.0	1.2	15.0%
	20	10	2	13.0	0.8	6.2%
6.0	2.5	20	0.125	-29.4	4.2	14.3%
	2.5	10	0.25	-31.2	2.5	8.0%
	5	10	0.5	-23.1	0.3	1.3%
	10	10	1	2.0	0.4	20.0%
	20	10	2	5.7	0.2	3.5%
7.0	2.5	20	0.125	-35.8	1.3	3.6%
	2.5	10	0.25	-33.2	3.5	10.5%
	5	10	0.5	-35.8	0.1	0.3%
	5	6.7	0.75	-13.9	0.8	5.8%
	10	10	1	-6.5	0.6	9.2%
	20	10	2	3.8	1.2	31.6%
8.0	5	10	0.5	-30.3	3.3	10.9%
	10	10	1	-1.5	1.9	126.7%
	20	10	2	3.2	1.1	34.4%

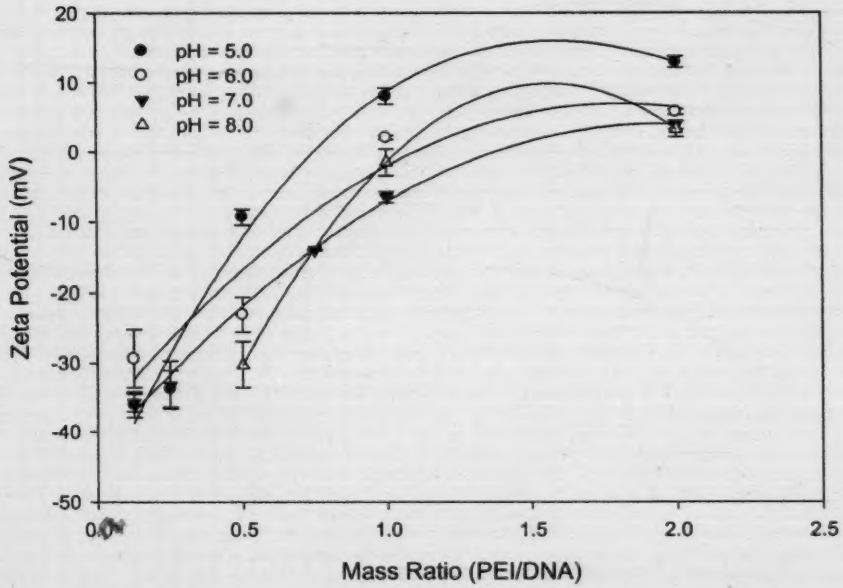

Figure 3-4A. The average zeta potential of PEI/linear DNA complexes in phosphate buffers with different pH values (5.0, 6.0, 7.0 and 8.0, NaCl concentration was 30 mM) as a function of PEI/linear DNA mass ratio. The results are shown as mean values (± SD) of 3 measurements.

Figure 3-4A shows the zeta potential of PEI/linear DNA complexes at different pH values as a function of PEI/linear DNA mass ratio. For PEI/linear DNA mass ratio at 0.5 to 2, the zeta potential increases as PEI/linear DNA mass ratio increases. For PEI/DNA mass ratio below 0.5, the zeta potential of the solutions was all around -30 mV to -40 mV. Compared to what we observed before, the slope of the curves was significantly smaller.

Table 3-4B summarized the results of the zeta potential measurements in 150 mM NaCl solutions at different pH. PEI to linear DNA ratios were controlled instead of the actual concentrations of PEI or DNA.

Table 3-4B. The characteristic of PEI/linear DNA samples used for zeta potential measurements and average zeta potential values of the PEI/linear DNA complexes in phosphate buffer (NaCl conc. =150 mM).

pH	PEI Conc. (μg/mL)	DNA Conc. (μg/mL)	PEI/DNA Mass Ratio	Mean Zeta Potential (mV)	SD (mV)	CV
5.0	1.875	15	0.125	-26.1	5.6	21.4%
	2.5	10	0.25	-34.9	2.9	8.3%
	5	10	0.5	-14.5	4.4	30.3%
	10	10	1	16.4	1	6.1%
	20	10	2	13.2	4.1	31.1%
6.0	2.5	10	0.125	-29.1	5.2	17.9%
	5	6.7	0.25	-30.4	5.6	18.4%
	5	10	0.5	-11.4	2.3	20.2%
	10	10	1	-2.5	3.4	136.0%
	20	10	2	9.8	3.5	35.7%

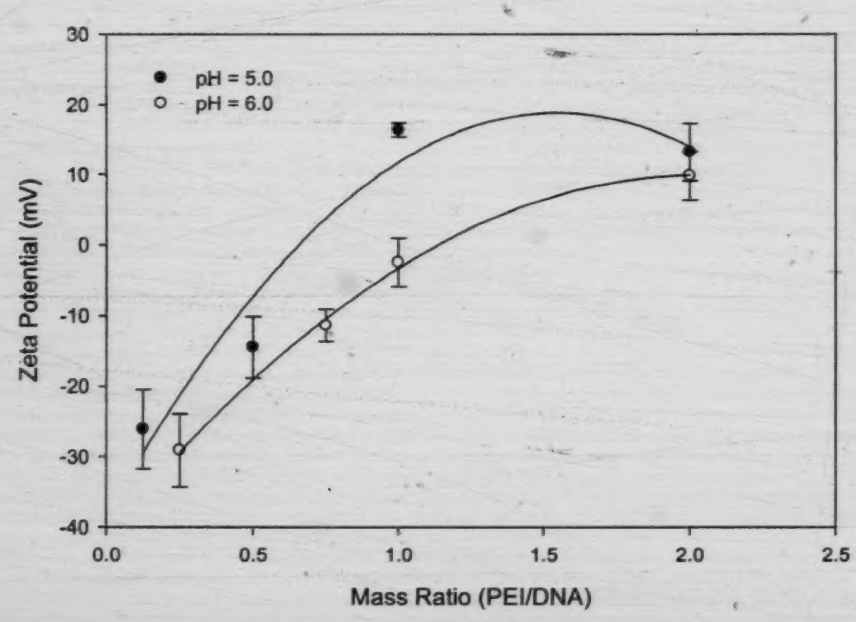

Figure 3-4B. The average zeta potential of PEI/linear DNA complexes in phosphate buffers with different pH values (NaCl concentration was 150 mM) as a function of PEI/linear DNA mass ratio. The results are shown as mean values (± SD) of 3 measurements.

Figure 3-4B shows the average zeta potential of the PEI/linear DNA complexes as a function of PEI/linear DNA mass ratio. For the first series where pH value equals 5.0, the zeta potential increased as PEI/linear DNA mass ratio increased from 0.125 to 1, and then slightly decreased when PEI/linear DNA mass ratio increased to 2. For the second series where pH value equals 6.0, the zeta potential increased gradually as PEI/DNA mass ratio increased. There was no decrease in zeta potential value when PEI/DNA mass ratio changed from 1 to 2. However the slope of increase was slightly smaller. Compared between these two series, the zeta potential values of those at pH=5.0 were higher than their counterpart at pH=6.0. When PEI/linear DNA mass ratio was 1, zeta potential value at pH=5.0 was significantly higher than the value at pH=6.0. Overall, they share the same trend as the previous set of experiments where NaCl concentration was lower at 30 mM.

4.2 Zeta Potential Distribution

Examining the average zeta potential values alone will sometimes miss the important information regarding to the heterocoagulation phenomena in the aqueous media. In order to better understand the actual status of the PEI/DNA complexes in the solution, zeta potential distribution was analyzed using the data obtained by the Zetasizer.

Figure 3-5 shows the zeta potential distribution of the complexes at various PEI to DNA ratios in 30 mM NaCl solution at pH 5.0. At PEI/DNA ratio equals to 0.125, the zeta potential distribution shown in Figure 3-5A had a board single peak centered at around -36 mV. At PEI/DNA ratio equal to 0.25, two narrower peaks in conjunction to each other were observed in zeta potential distribution shown in Figure 3-5B. The one

with higher intensity was peaked around -50 mV and the other was peaked around -15 mV. When PEI/linear DNA ratio changed to 0.5 in Figure 3-5C, the zeta potential distribution shifted significantly towards positive, while it still featured two peaks with similar intensity at around -30 mV and 5 mV respectively. At PEI/linear DNA ratio equals to 1, the zeta potential distribution single peaked around 8 mV as shown in Figure 3-5D. In Figure 3-5E, the single peak shifted to around 13 mV in zeta potential distribution diagram when PEI/linear DNA ratio increased to 2.

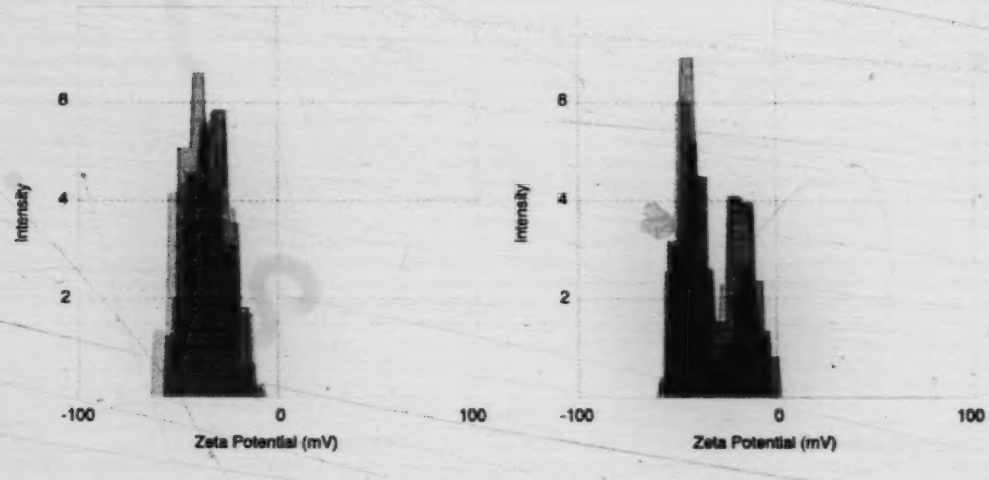

(A) (B)

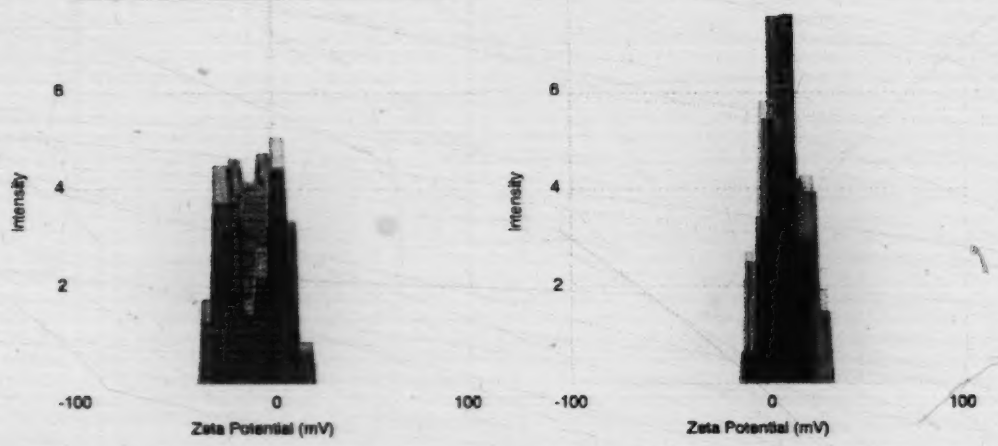

(C)

(D)

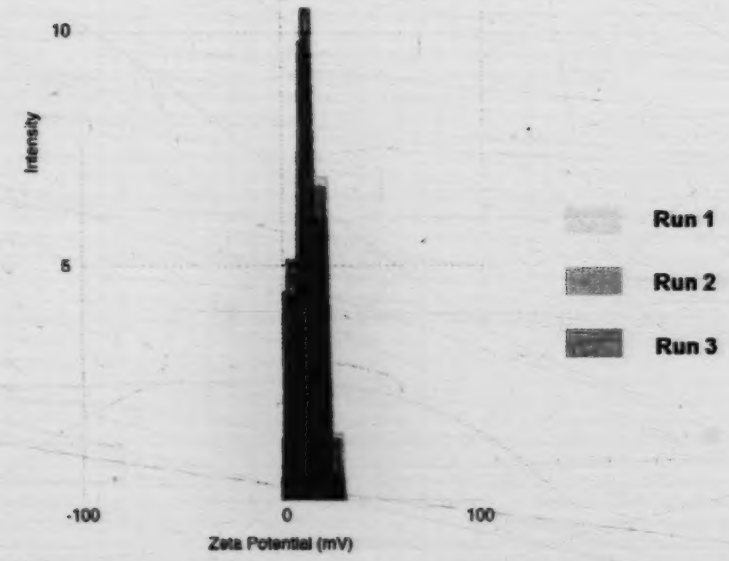

(E)

Figure 3-5. The zeta potential distributions for PEI/linear DNA complexes at pH 5.0 in 30 mM NaCl solution. PEI/linear DNA mass ratio is: (A) 0.125; (B) 0.25; (C) 0.5; (D) 1 and (E) 2.

4.3 Size Measurement

PCS analysis was used to determine the size of the complexes, and it was performed on the Zetasizer equipped with 10 mW HeNe laser. Scattering light was detected at 90° angle through a 400 μm pinhole at 25 °C. The sampling time was set to 5 min and each run consisted of 10 subruns.

4.3.1 PEI/PAA Complexes in H_2O

The first series of size measurement was focused on PEI/PAA complexes. The PEI concentration for all the samples were maintained at 10 μg/mL while the PAA concentration varied accordingly to set the PEI to PAA mass ratio to be 0.33, 0.5, 1, 2 and 3. The results of the size measurements of PEI/PAA complexes are summarized in Table 3-5.

Table 3-5. The characteristic of PEI/PAA samples used for size measurements and average size of the PEI/PAA complexes in H_2O. The samples used in this experiment are the same as the samples in part of Table 3-1.

PEI Conc. (μg/mL)	PAA Conc. (μg/mL)	PEI/PAA Mass Ratio	Average Size (nm)	SD (nm)	CV
10	30	0.33	469.8	20.3	4.3%
10	20	0.5	557.8	13.1	2.4%
10	10	1	505.4	12.4	2.4%
10	5	2	395.0	12.2	3.1%
10	3.3	3	466.3	16.7	3.6%

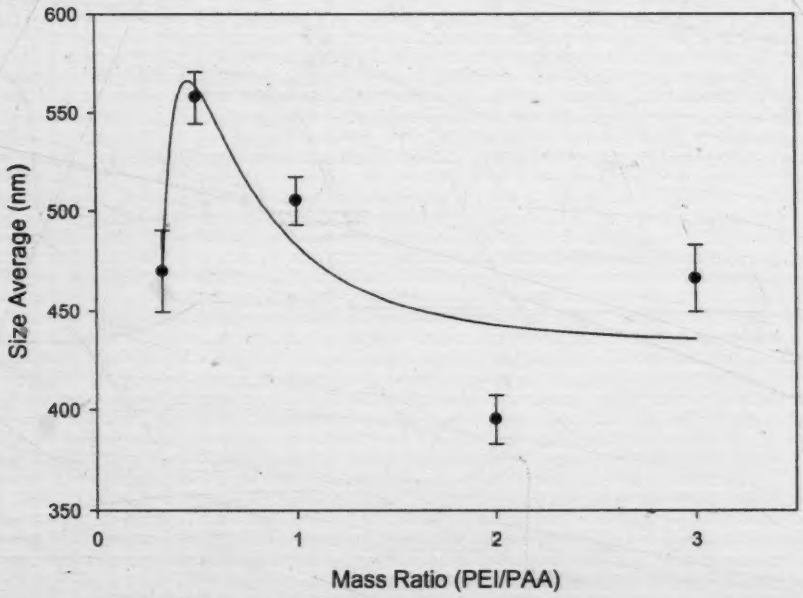

Figure 3-6. The average size of PEI/PAA complexes in H_2O as a function of PEI/PAA mass ratio. The results are shown as mean values (± SD) of 3 measurements.

Figure 3-6 shows the size of the PEI/PAA complexes change as a function of PEI/PAA mass ratio. The results show that initially the size of the complexes slightly increased as the PAA concentration decreased until it reached the peak at PEI to PAA mass ratio equaled to 0.5. Then the size decreased as the PAA concentration decreased, and finally stabled around 400 nm. With a relatively small standard deviation, the results were reproducible. The reason why PEI to PAA mass ratio at 0.5 gave the largest size is probably because of the fact that the zeta potential of the complexes was close to neutrality, and that would likely result in an aggregation of the complexes. (See Figure 3-1)

4.3.2 PEI/Linear DNA Complexes in H_2O

With the encouraging PCS results obtained from PEI/PAA, we changed our focus onto PEI/DNA complexes. The first set of experiments was performed in H_2O. Two different series of samples were examined, a) The PEI concentrations were maintained at 5 μg/mL while the linear DNA concentrations were varied so that the mass ratios of PEI to linear DNA were 0.1, 0.2, 0.25, 0.5 and 1; b) The linear DNA concentrations were maintained at 5 μg/mL while the PEI concentrations were varied so that the mass ratios of PEI to linear DNA were 0.1, 0.2, 0.25, 0.5 and 1. The reason for choosing these two series of samples was to explore whether it was the PEI to linear DNA mass ratio instead of the absolute concentration of PEI and linear DNA that determined the size of the complexes. The result of the size measurements of PEI/linear DNA complexes in H_2O are summarized in Table 3-6.

PEI Conc. (μg/mL)	DNA Conc. (μg/mL)	PEI/DNA Mass Ratio	Average Size (nm)	SD (nm)	CV
5	50	0.1	92.0	3.2	3.4%
5	25	0.2	173.0	1.2	0.7%
5	20	0.25	243.0	17.0	7.0%
5	10	0.5	146.0	1.3	0.9%
5	5	1	135.0	0.7	0.5%
0.5	5	0.1	122.9	8.7	7.1%
0.625	5	0.125	133.9	1.7	1.3%
0.83	5	0.167	137.2	0.8	0.6%
1.25	5	0.25	246.3	4.8	1.9%
1.67	5	0.33	183.8	3.0	1.6%
5	5	1	114.0	6.0	5.3%

Table 3-6. The characteristic of PEI/linear DNA samples used for size measurements and average size of the PEI/linear DNA complexes in H_2O. Some of the samples used in this experiment (PEI concentrations are 5 μg/mL) are the same as the samples in part of Table 3-2.

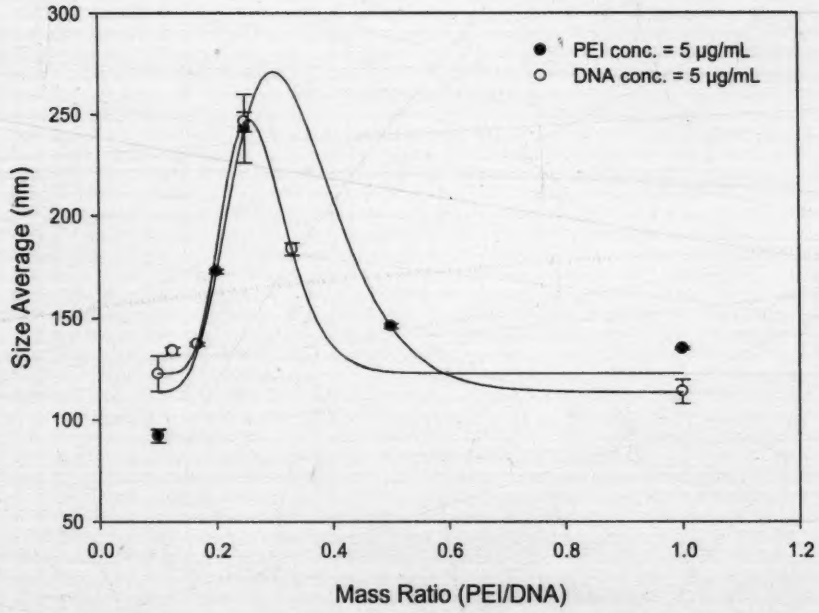

Figure 3-7. The average size of PEI/linear DNA complexes in H_2O as a function of PEI/linear DNA mass ratio. The results are shown as mean values (± SD) of 3 measurements. Where no standard deviation is visible, they are smaller than the symbols used.

Figure 3-7 shows the size of the PEI/linear DNA complexes in H_2O as a function of PEI/linear DNA mass ratio. Similar to PEI/PAA results in Figure 3-5, initially the size of the complexes increased as the PEI/linear DNA mass ratio increased until it reached the peak. The difference is that the mass ratio at the peak was at 0.25 instead of at 0.5. Then the size decreased as the PEI/linear DNA mass ratio further increased. The size of the complexes at both low end and high end were around 100 to 150 nm, and the size at the 0.25 mass ratio were about 245 nm for both series of samples. The standard deviation and coefficient of variation were small for most of the samples, which means the results were reproducible. Compared with previous zeta potential results for this set of samples

(See Figure 3-2), the results correlated well with each other as the zeta potential of the complexes was close to neutrality at the PEI to PAA mass ratio equal to 0.25. Larger particle size at this ratio might result from an aggregation of the complexes due to lack of repulsives force between the complexes.

4.3.3 PEI/Linear DNA Complexes in NaCl Solution

The ionic strength of the solution used for complex formation was changed by adding NaCl to the solution. Size measurement of PEI/linear DNA complexes with the PEI to linear DNA mass ratio at 0.25, 0.5, 1 and 2 was performed in 30 mM and 150 mM NaCl solutions. For samples with PEI to DNA mass ratio at 0.25, 0.5, 1 and 2, the DNA concentrations were maintained at 10 μg/mL. For samples with PEI to linear DNA mass ratio at 0.125, the linear DNA concentration of the samples was increased to 15 μg/mL to keep the Zetasizer's count rate in the optimal range. The PEI concentration of each samples were varied according to the linear DNA concentration to maintain the PEI to linear DNA mass ratio at certain values. The results of the size measurements of PEI/linear DNA complexes in NaCl are summarized in Table 3-7.

Figure 3-8 shows the size of the PEI/DNA complexes in NaCl solutions as a function of PEI/DNA mass ratio. Four main findings were evident from this figure: 1) The size of the complexes initially increased as the PEI/DNA mass ratio increased from approximately 120 nm to above 1000 nm until it reached the peak at PEI to DNA mass ratio equal to 0.5. Then the size decreased to 110 – 120 nm level as the DNA concentration decreased. 2) The standard deviation was very small for almost all the samples, which means the results were quite reproducible. 3) The largest and smallest

complex size for each series were similar to each other, which indicates that the concentration of NaCl did not affect the change of the particle size in the range of 30 mM to 150 mM. 4) The position where the peak located was consistent with zeta potential results as at mass ratio equal to 0.5, the zeta potential of the complexes was close to zero.

Table 3-7. The characteristic of PEI/linear DNA samples used for size measurements and average size of the PEI/linear DNA complexes in NaCl. The samples used in this experiment are the same as the samples in part of Table 3-3.

NaCl Conc. (mM)	PEI Conc. (μg/mL)	DNA Conc. (μg/mL)	PEI/DNA Mass Ratio	Average Size (nm)	SD (nm)	CV
30	1.875	15	0.125	120.5	1.9	1.6%
	2.5	10	0.25	149.2	3.1	2.1%
	5	10	0.5	1200.8	22.4	1.9%
	10	10	1	167.2	2.7	1.6%
	20	10	2	129.9	0.6	0.5%
150	1.875	15	0.125	115.2	3.2	2.8%
	2.5	10	0.25	305.3	1.8	0.6%
	5	10	0.5	1281.9	14.7	1.1%
	10	10	1	144.9	1.2	0.8%
	20	10	2	110.6	3.5	3.2%

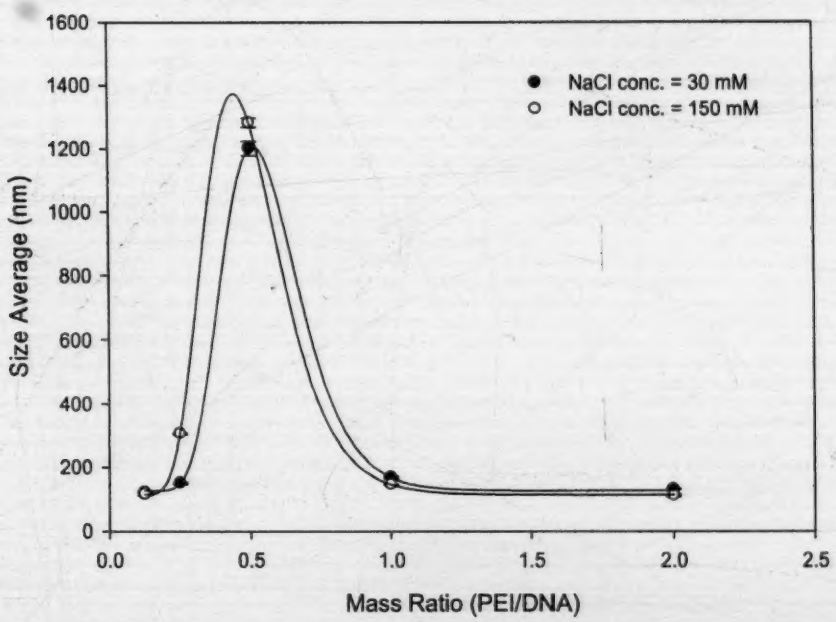

Figure 3-8. The average size of PEI/linear DNA complexes in NaCl as a function of PEI/DNA mass ratio. The results are shown as mean values (± SD) of 3 measurements. Where no standard deviation is visible, they are smaller than the symbols used.

4.3.4 PEI/Linear DNA Complexes in Phosphate Buffer

To study the pH effect on particle size of PEI/linear DNA complexes, size measurements were performed in phosphate buffers of different pHs. NaCl concentrations were maintained at 30 mM and 150 mM, respectively. For NaCl concentration at 30 mM, four series of samples with pH value at 5.0, 6.0, 7.0 and 8.0 were examined. Table 3-8 A summarizes the results of the size measurements in 30 mM NaCl solutions at different pH.

Figure 3-9 A shows the size of the PEI/DNA complexes in phosphate buffer solutions as a function of PEI/linear DNA mass ratio. Four main observations are: 1) The

size of the PEI/linear DNA complexes did not change significantly when the PEI to linear DNA mass ratio changed from 0.125 to 0.25 for each series of samples at different pH. At pH=5.0, the size of the complexes was larger than those at pH=6.0, 7.0 and 8.0. 2) For pH=5.0, 6.0 and 8.0 series, the size of the complexes increased significantly when the mass ratio changed from 0.25 to 0.5, and decreased when the mass ratio changed from 0.5 to 1.0 and above. Compared to the other three series, the size of the complexes at pH=7.0 gradually increased when the mass ratio changed from 0.25 to 1.0, and slightly decreased when the mass ratio changed from 1.0 to 2.0. No significant size peak observed for pH=7.0 series. 3) Unlike previous sets of experiments, the size of the complexes at the high mass ratio ends was significantly larger than the size at low end. 4) The results of size measurements were not as consistent with the results of zeta potential measurements as with previous sets of experiments in which the largest sizes appeared in the area where the zeta potential of the complexes was nearly zero. (See Figure 3-4 A) The presence of phosphate buffer which would reduce the positive charge on particles appears to be the reason. The reduced charge promotes particle aggregation increasings the particle size substantially.

Table 3-8A. The characteristic of PEI/linear DNA samples used for size measurements and average size of the PEI/linear DNA complexes in phosphate buffer (NaCl conc. =30 mM). The samples used in this experiment are the same as the samples in part of the Table 3-4A.

pH	PEI Conc. (μg/mL)	DNA Conc. (μg/mL)	PEI/DNA Mass Ratio	Average Size (nm)	SD (nm)	CV
5.0	2.5	20	0.125	410.0	7.3	1.8%
	2.5	10	0.25	412.5	0.5	0.1%
	5	10	0.5	1641.2	42.1	2.6%
	10	10	1	1084.9	22.1	2.0%
	20	10	2	987.8	28.3	2.9%
6.0	2.5	20	0.125	175.6	6.2	3.5%
	2.5	10	0.25	182.0	2.2	1.2%
	5	10	0.5	2129.0	149.9	7.0%
	10	10	1	1467.6	27.2	1.8%
	20	10	2	1342.7	30.3	2.2%
7.0	2.5	20	0.125	275.4	2.6	0.9%
	2.5	10	0.25	286.1	7.6	2.6%
	5	10	0.5	339.2	2.0	0.6%
	5	6.7	0.75	772.3	21.9	2.8%
	10	10	1	1165.5	17.7	1.5%
	20	10	2	965.9	37.7	3.9%
8.0	2.5	20	0.125	150.1	7.0	4.7%
	2.5	10	0.25	126.4	2.2	1.7%
	5	10	0.5	1314.2	57.5	4.4%
	10	10	1	1086.8	3.6	0.3%
	20	10	2	970.8	57.3	5.9%

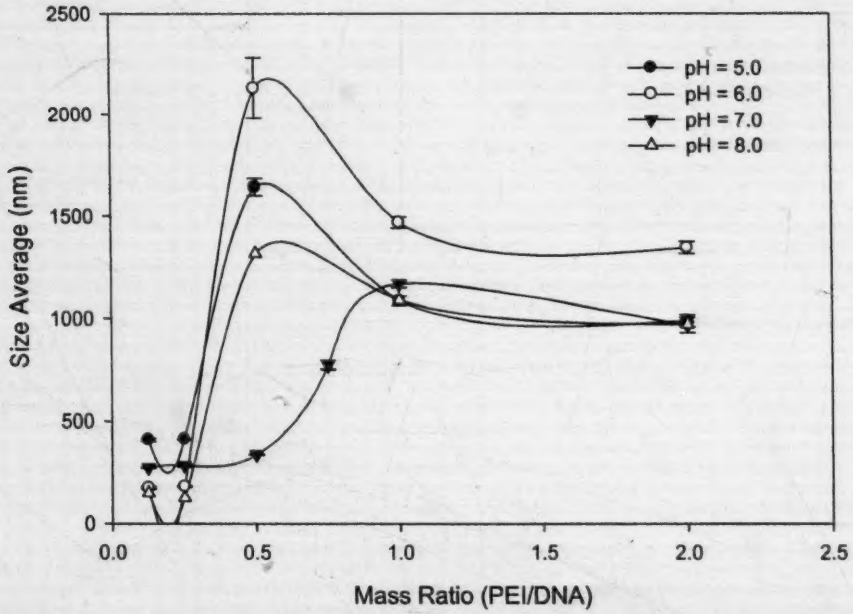

Figure 3-9A. The average size of PEI/linear DNA complexes in phosphate buffers with different pH values (5.0, 6.0, 7.0 and 8.0, NaCl concentration was 30 mM) as a function of PEI/linear DNA mass ratio. The results are shown as mean values (± SD) of 3 measurements. Where no standard deviation is visible, they are smaller than the symbols used.

For NaCl concentration at 150 mM, two series of samples with pH value at 5.0 and 6.0 were examined. Table 3-8 B summarizes the results of the size measurements on Zetasizer in 150 mM NaCl solutions at different pH. Figure 3-9 B shows the size of the PEI/linear DNA complexes in phosphate buffer solution as a function of PEI/linear DNA mass ratio. For pH=5.0 series, the size of complexes initially increased as DNA concentration decreased when PEI to linear DNA mass ratio changed from 0.125 to 0.5. The size of the complexes was at its largest when PEI to linear DNA mass ratio was equal to 0.5, then it decreased as linear DNA concentration decreased and finally leveled off at around 1000 nm. For pH=6.0 series, there was no peak in size. Initially, the size of

the complexes was around 300 to 400 nm when PEI to linear DNA mass ratio changed from 0.25 to 0.5. Then, it significantly increased as the mass ratio increased. After the mass ratio reached 1, the complexes size leveled off at around 1000 nm. Similar to what had happened in phosphate buffer with 30 mM NaCl concentration, the complexes at the high mass ratio ends was significantly larger than the size at low end. And again, the mass ratio at which the size of the complexes was the largest was not at the condition where the zeta potential of the complexes was close to zero. (See Figure 3-4 B)

Table 3-8B. The characteristic of samples used for size measurements and average size of the PEI/linear DNA complexes in phosphate buffer (NaCl conc. =150 mM). The samples used in this experiment are the same as the samples in part of the Table 3-4B.

pH	PEI Conc. (μg/mL)	DNA Conc. (μg/mL)	PEI/DNA Mass Ratio	Average Size (nm)	SD (nm)	CV
5.0	1.875	15	0.125	288.6	45.61	15.8%
	2.5	10	0.25	220.2	12.02	5.4%
	5	10	0.5	1380.9	202.80	14.7%
	10	10	1	1093.2	3.96	0.4%
	20	10	2	1041.1	30.83	3.0%
6.0	2.5	10	0.125	387.2	3.04	0.8%
	5	6.7	0.25	275.7	23.12	8.4%
	5	10	0.5	923.2	26.45	2.9%
	10	10	1	1139.5	41.44	3.6%
	20	10	2	1037.1	17.25	1.7%

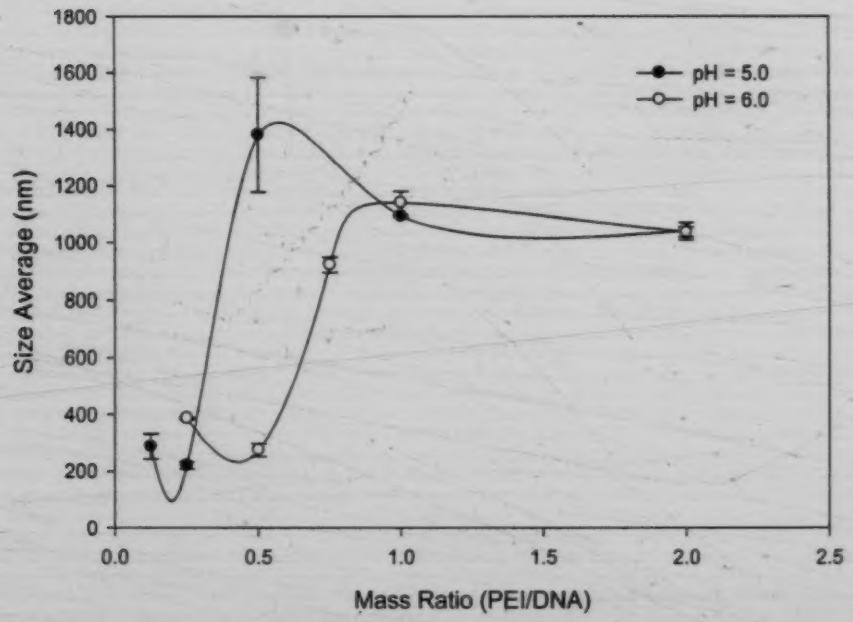

Figure 3-9B. The average size of PEI/linear DNA complexes in phosphate buffers with different pH values (5.0 and 6.0, NaCl concentration was 150 mM) as a function of PEI/DNA mass ratio. The results are shown as mean values (± SD) of 3 measurements. Where no standard deviation is visible, they are smaller than the symbols used.

4.4 AFM Imaging

The PEI/DNA complexes were characterized by tapping mode atomic force microscopy.

4.4.1 Correlation of AFM Imaging and PCS

As a validation of the technique, PEI/linear DNA complexes were firstly examined using AFM. The linear DNA concentration was maintained at 30 μg/mL and 10 μg/mL in two different series and PEI concentration were varied accordingly to set the PEI to linear DNA mass ratio at 0.125, 0.25, 0.5, 1 and 2. For the series with the linear DNA concentration at 30 μg/mL, there were too many particles collapse with each other,

which indicated that the concentration of the particles was too high. For linear DNA concentration at 10 μg/mL series, particles were better defined. The AFM images for PEI/linear DNA complexes at different PEI/DNA ratios are shown in Figure 3-10. When PEI/linear DNA mass ratio was at 0.125, few big particles coexisted with smaller particles as shown in Figure 3-10A. Some rod-like structures were also observed in the background. When PEI/linear DNA mass ratio was at 0.25, few particles were observed and most of them were similar to the size of the one shown in Figure 3-10B. As PEI/linear DNA mass ratio increased to 0.5, large quantity of smaller particles were shown in AFM image (Figure 3-10C). When PEI/linear DNA mass ratio was at 1, both big particles and small particles were observed (Figure 3-10D). No significant difference was observed in terms of particle size and quantity when PEI/linear DNA mass ratio increased to 2 (Figure 3-10E). The AFM results of the size of PEI/linear DNA complexes are summarized in Table 3-9.

PEI/DNA Mass Ratio	Mean Size (nm)	Min Size (nm)	Max Size (nm)	SD (nm)	CV
0.125	106	75	177	22	12.4%
0.25	141	82	226	56	24.8%
0.5	98	65	152	19	12.5%
1	119	85	233	33	14.2%
2	101	61	197	32	16.2%

Table 3-9. The AFM results of the size of PEI/linear DNA complexes in H_2O. Mean sizes were calculated from 25 particles per sample except for samples with PEI/linear DNA mass ratio equal to 0.25 in which case only 10 particles were used to calculate mean size.

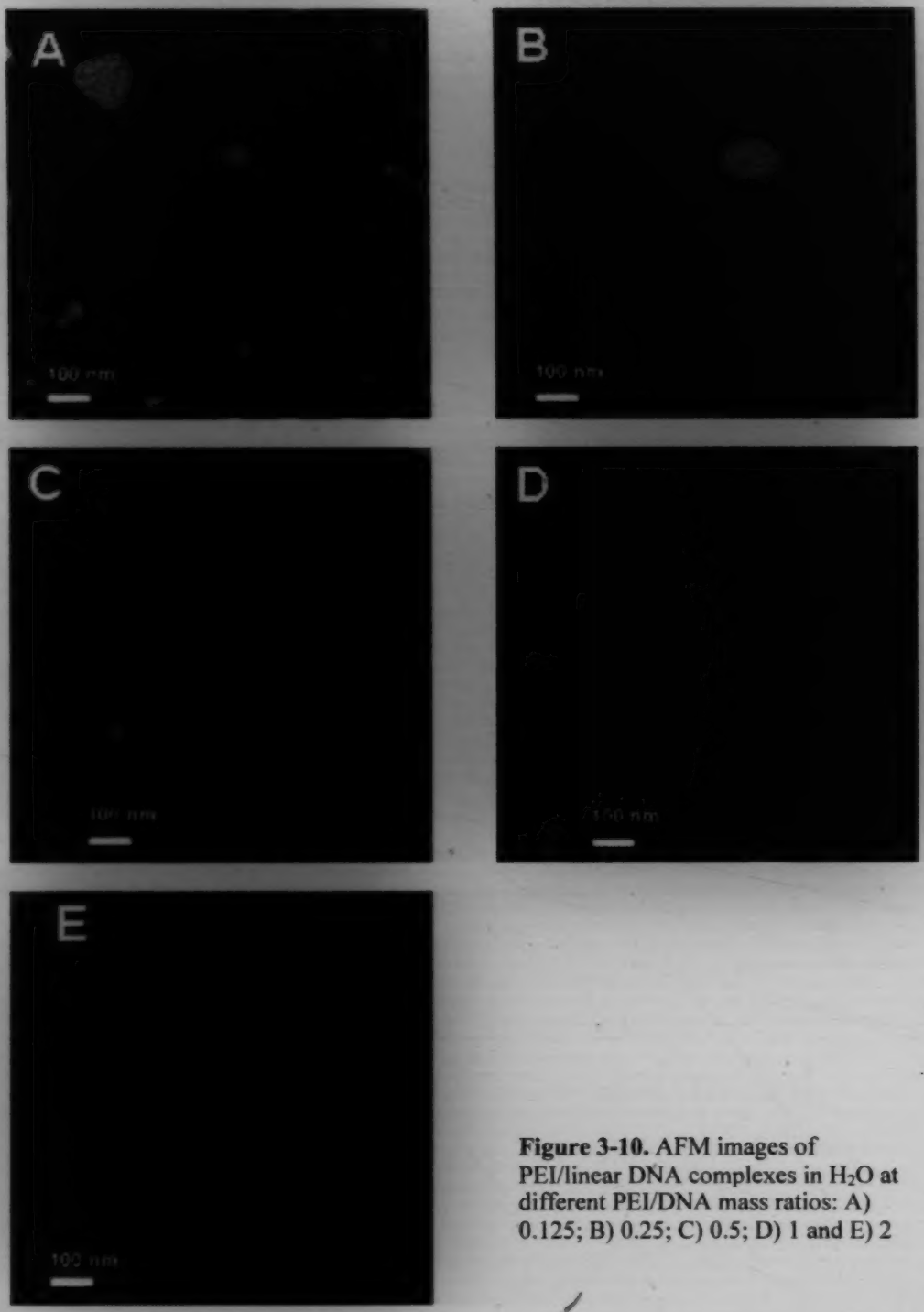

Figure 3-10. AFM images of PEI/linear DNA complexes in H_2O at different PEI/DNA mass ratios: A) 0.125; B) 0.25; C) 0.5; D) 1 and E) 2

Figure 3-11 shows the size of the complexes obtained from AFM images as a function of PEI/linear DNA mass ratio. Three main findings are notable from this figure: 1) Similar to previous PCS results (See Figure 3-7), the largest mean size of the PEI/DNA complexes appeared at the mass ratio equal to 0.25. Particle size increased as mass ratio increased when it was lower than 0.25 and decreased as mass ratio increased when it was higher than 0.25. 2) At the mass ratio equaled to 0.5, the mean size of the complexes was the smallest. 3) Generally, particle size measured by PCS was somewhat larger than its counterpart measured by AFM. But the trends of change were similar to each other.

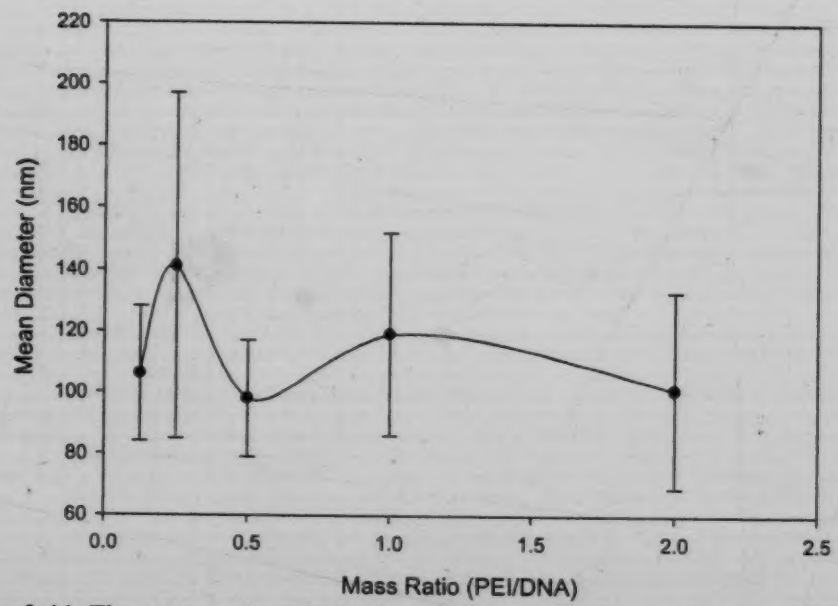

Figure 3-11. The average size of PEI/linear DNA complexes obtained from AFM images at different PEI/linear DNA mass ratio in H_2O.

4.4.2 AFM Imaging of Plasmid DNA

Since AFM requires much less sample than the Zetasizer, plasmid DNA was used to visualize the actual particle formation. Naked plasmid DNA was then prepared for AFM imaging. Firstly, plasmid DNA samples were prepared in H_2O at the concentration of 5 μg/mL (Figure 3-12A). According to section analysis, the width of the plasmid DNA was 24.5 nm and the height of the plasmid was 2.062 nm. Then, we prepared the DNA in 3 mM NaCl solution to help the attachment of DNA on negatively charged mica surface. Figure 3-12B shows NaCl particles ranging from 11.504 nm to 22.856 nm in diameter in the background. The section analysis results indicated that the length of the DNA was approximately 600 nm, the width of the DNA was 22.430 nm and the height of the DNA was 0.881 nm.

(A)

(B)

Figure 3-12. AFM images of plasmid DNA (pEGFP): (A) pEGFP in H_2O and (B) pEGFP in 3 mM NaCl solution.

4.4.3 Investigation of Complex Formation using AFM

In order to have a better understanding of the complex formation process, we performed a kinetic study of PEI/DNA complexation. PEI and plasmid DNA were thoroughly mixed and at each of the three different time points, 10 µL of the sample was transferred to mica disks and prepared for AFM imaging. The AFM images of these samples were then obtained and compared.

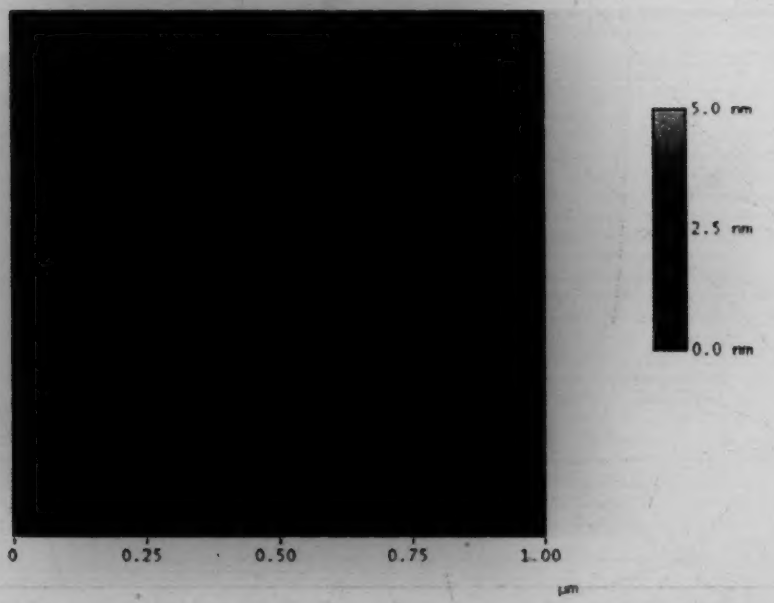

(A)

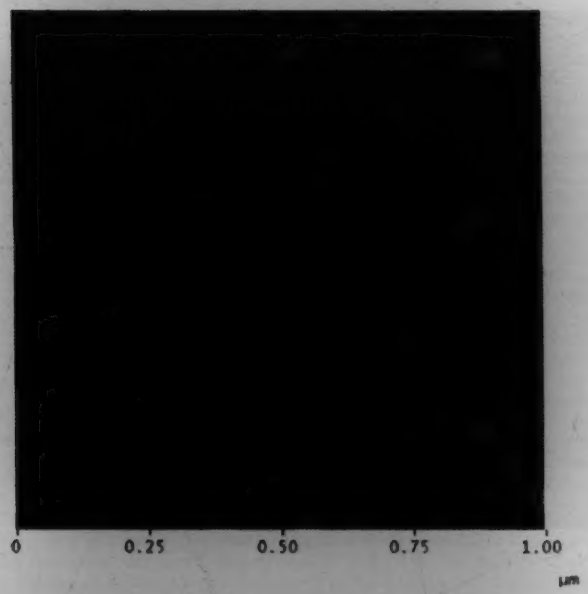

(B)

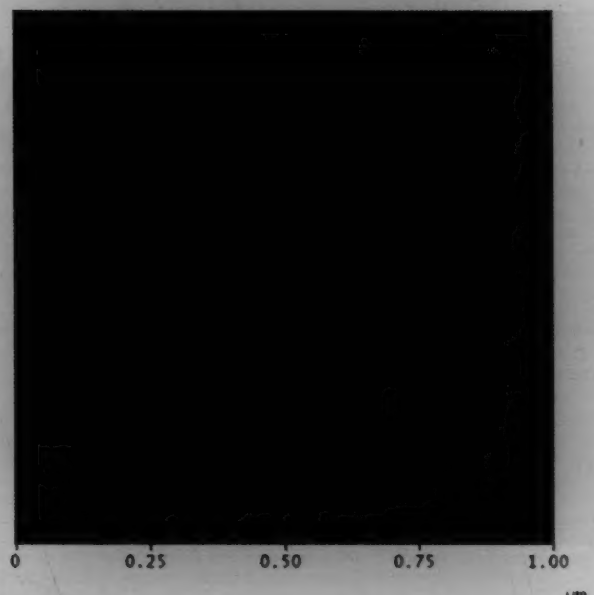

(C)

Figure 3-13. AFM images of PEI/DNA complexes at different complexation time: A) 1 minute; B) 10 minutes and C) 30 minutes.

Figure 3-13 shows the AFM images of PEI/DNA complex formation process at 1, 10 and 30 minutes after mixing. At one minute (Figure 3-13A), there was no PEI/DNA complex formed. PEI and DNA formed a linear network. The ribbon-like complexes were not evenly distributed on mica. There were locations with higher concentration of the complexes and the tendency of forming knots in some locations. The width of the ribbons was around 15 nm. At 10-minute time point (Figure 3-13B), PEI and DNA formed tadpole-shaped particles. The size of the particles was around 51 nm (min 35.272 nm, max 71.718 nm) and the width of the tails was around 27 nm. At 30-minute time point (Figure 3-13C), circular particles were formed and some of the small particles were beginning to aggregate to form larger particles.

4.4.4 AFM Imaging of PEI/Plasmid DNA Complexes in 3 mM NaCl

With a better understanding of the process of the complex formation, we then started another set of experiment to see the change of particle size at different PEI to plasmid DNA mass ratio. Plasmid DNA concentration of each sample was 2.5 μg/mL. PEI concentrations were varied and PEI/plasmid DNA mass ratios were maintained at 0.125, 0.25, 0.5, 1 and 2. At first, 30 mM NaCl buffer was used, but there were a lot of sub-40 nm particles in AFM images, which were believed to be NaCl crystals. In order to optimize the signal to noise ratio, we then decreased the NaCl concentration to 3 mM. The AFM images of PEI/plasmid DNA complexes at different PEI/plasmid DNA mass ratios were shown in Figure 3-14.

When PEI/DNA mass ratio was at 0.125, few particles were observed as shown in Figure 3-14A. When PEI/plasmid DNA mass ratio increased to 0.25, more particles were

observed as globular shape (See Figure 3-14B). As PEI/plasmid DNA mass ratio increased to 0.5, the particle size of PEI/plasmid DNA complexes increased significantly as seen in Figure 3-14C. When PEI/plasmid DNA mass ratio was at 1, the particle size was dropped noticeably (Figure 3-10D). No significant difference was observed in terms of particle size and quantity when PEI/plasmid DNA mass ratio increased to 2 (Figure 3-10E). After processing the AFM images using the Nanoscope III software, detail results of the size of PEI/plasmid DNA complexes are summarized in Table 3-10.

Table 3-10. The AFM results of the size of PEI/plasmid DNA complexes in 3mM NaCl. Mean sizes were calculated from 10 particles per each sample.

PEI/DNA Mass Ratio	Mean Size (nm)	Min Size (nm)	Max Size (nm)	SD (nm)	CV
0.125	245	194	278	26	9.4%
0.25	189	146	215	27	12.6%
0.5	361	294	462	58	12.6%
1	178	140	235	29	12.3%
2	102	73	146	27	18.5%

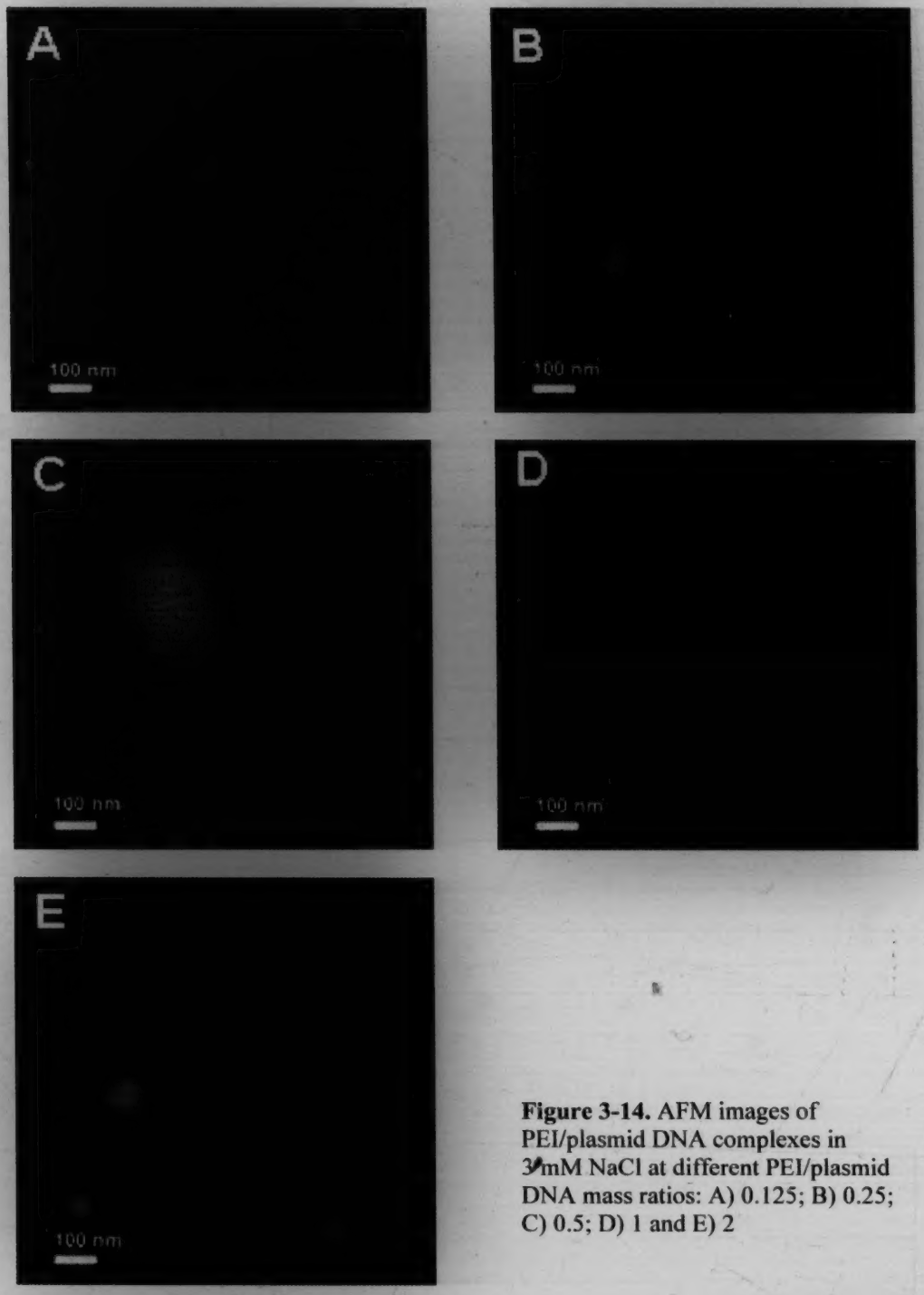

Figure 3-14. AFM images of PEI/plasmid DNA complexes in 3 mM NaCl at different PEI/plasmid DNA mass ratios: A) 0.125; B) 0.25; C) 0.5; D) 1 and E) 2

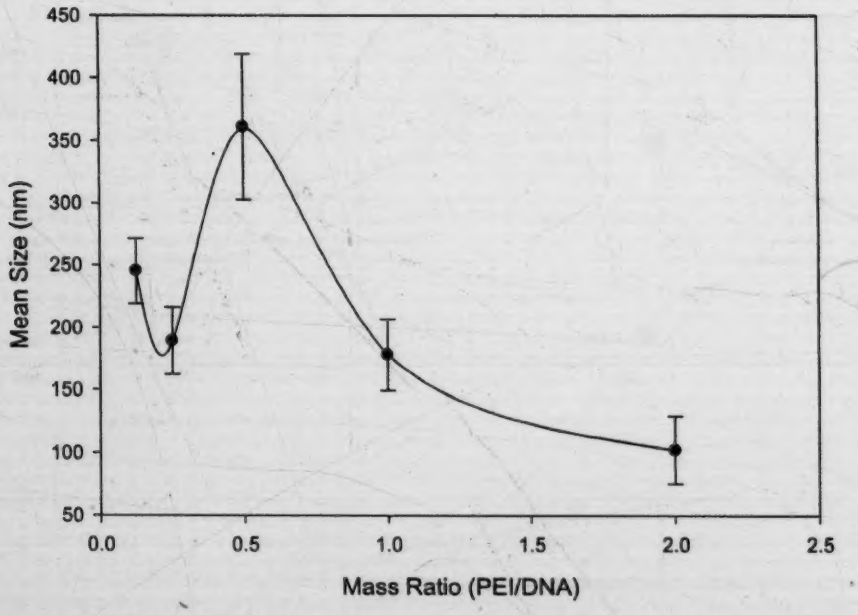

Figure 3-15. The average size of PEI/plasmid DNA complexes at different mass ratio in 3mM NaCl.

Figure 3-15 shows the average size of PEI/plasmid DNA complexes in 3 mM NaCl as a function of PEI to DNA mass ratio. At lower PEI/plasmid DNA mass ratios, particle size was around 230 nm and did not change significantly until the PEI/DNA mass ratio reached 0.5 where the particle size reached a maximum of around 350 nm. At higher PEI/plasmid DNA mass ratio, particle size decreased dramatically as PEI/plasmid DNA mass ratio increased. The final particle size was around 100 nm when PEI/plasmid DNA mass ratio increased to 2.

5. DISCUSSION

We determined some of the biophysical properties of the interactions between DNA and cationic polymers, specifically PEI, as gene carrier. The results will not only help us further understand the complexation process, but also give us valuable guidance on designing novel carriers for gene delivery.

Our hypothesis was that the interactions between cationic polymers and DNA were primarily electrostatic in nature. At first, we used negatively charged PAA as a model of plasmid DNA in zeta potential measurements. The results of average zeta potential for PEI/PAA complexes allowed us to understand the electrokinetic behavior (or the zeta potential) of the binary mixture system. There was no significant difference in zeta potential value at each mass ratio point between the series of 5 μg/mL and 10 μg/mL PEI. From this finding, we determined 5 μg/mL to be the PEI concentration used in the next PEI/linear DNA study. Although the charge per mass value of PAA was different from those of the DNA molecules because of the composition and structural differences, the results obtained with PEI/linear DNA showed the similar trend as those obtained with PEI/PAA as a function of mass ratio. The main difference is that the mass ratios at which the zeta potential of the particles were close to neutrality were around 0.5 to 0.75 for PEI/PAA, while it was about 0.25 for PEI/linear DNA. These results indicate that DNA molecules hold more negative charges than PAA at the same concentration. This is confirmed by different pK_a values of around 1.5 [46] and 5.0 [47] for DNA's phosphate groups and PAA, respectively. When the complexes have either a high negative or positive zeta potential, the size of the complexes is relatively small (See

Figure 6). However, when the zeta potential approaches neutrality, the size of the complexes increases drastically presumably due to aggregation of the complexes.

It was previously reported that high ionic strength would adversely affect the cationic polymer-DNA binding [16]. Tang *et al.* used the relative ethidium bromide fluorescence to measure the effect of NaCl concentration on binding affinity between plasmid DNA and different cationic polymers (polylysine, intact dendrimer, fractured dendrimer and polyethylenimine). In our study, we added NaCl to increase the ionic strength in order to see if it would affect the zeta potential of the complexes. Comparing Figure 3-2 with Figure 3-3, we can see that the mass ratio of PEI/linear DNA at which the zeta potential of the complexes reached zero seemed to be increasing as the NaCl concentration increased from 0 to 30, and then150 mM. Compared to zeta potential of PEI/linear DNA complexes in H_2O (33.6 mV to 46.8 mV, see Figure 3-2), the corresponding zeta potential of the PEI/linear DNA complexes in NaCl buffer was relatively lower (9.4 mV to 28.9 mV, see Figure 3-3) at PEI/linear DNA mass ratio higher than 0.5, i.e. when PEI/linear DNA complexes held a positive zeta potential. These results indicate that excessive ions in the solution posed a charge shielding effect on the particles in the solution, reducing the repulsive force between particles and, therefore, leading to aggregation of PEI/DNA complexes. A significant increase in the average particle size of PEI/DNA complexes in NaCl buffer (See Figure 3-8) than in H_2O (See Figure 3-7) was indeed observed. The size of the complexes in NaCl buffer was significantly bigger than that in H_2O when zeta potential of the complexes was close to zero. When zeta potential was strongly negative or positive, the size of the complexes in both NaCl buffer and in H_2O was similar. It is therefore, safe to come to the conclusion

that high ionic strength promotes aggregation of the particles in the solution. It was also reported by Oupicky *et al.* that the presence of NaCl promoted aggregation, thus cluster size was highly dependent on ionic strength for multi-DNA interpolyelectrolyte complexes [48, 49].

We introduced phosphate buffer to control the pH of the solution and examine the change of biophysical properties of PEI/linear DNA complexes at different pH values. It was reported that within pH range investigated in our study, pKa of DNA's phosphate groups was around 1.5 [46], and no denaturation of the DNA structure occured [50]. From Figure 3-4A and Figure 3-4B, we can see that the presence of phosphate affected the zeta potential of the complexes at all pH values significantly. At low PEI/DNA mass ratio, zeta potential values were around -25 mV to -35 mV, similar to the values we obtained earlier, in the absence of phosphate. As PEI/linear DNA mass ratio increased, zeta potential of the complexes in phosphate buffer increased much slower than observed in early studies using H_2O and NaCl buffers, exhibiting much smaller zeta potential values at the high PEI/linearDNA mass ratio end. A noticeable shift towards higher value in PEI/linear DNA mass ratio at which the zeta potential close to neutrality was also observed. This shift can not be simply explained by the change of ionic strength because we did not observe any significant change in that ratio when measured in H_2O and in NaCl buffers. This is more likely to be a result of the complicated heterocoagulation phenomena within the solution, which are usually ignored when analyzing average zeta potential values alone. Zeta potential distribution analysis helped us further understand the status of PEI and linear DNA in the solution. In Figure 3-5A, the single peak was strongly negative, indicating an insufficient amount of PEI in the

solution to fully neutralize the negatively charged linear DNA. With increasing PEI/linear DNA mass ratio, two peaks appeared in zeta potential distribution diagram. This observation suggests the presence of two different kinds of particles coexisting in the solution (See Figure 3-5B). It appears that part of the linear DNA molecules were neutralized by cationic polymers while the remaining part the linear DNA molecules stayed almost unneutralized. In Figure 3-5C, both of the peaks were shifted towards positive direction as a result of better PEI neutralization of linear DNA. In this case, part of the PEI/linear DNA complexes was already neutralized. With further increase in PEI addtion to the solution, PEI/linear DNA complexes were fully neutralized as shown in Figure 3-5D, merging the two zeta potential distribution peaks into one at around zero. Finally, when excessive PEI was present, one narrow positive peak appeared in the zeta potential distribution diagram, indicating a strong attraction between PEI and linear DNA. Similar changing patterns of zeta potential distribution were observed in several other series of experiment in phosphate buffer at different pHs. The particle size of those PEI/linear DNA complexes at low PEI/linear DNA mass ratio was relatively small. At high PEI/linear DNA ratio, however they were 2.4 to 7.6 times larger. Godbey *et al.* claimed that the pH of PEI solutioins had no discernible effect on transfection [51].

To further investigate biophysical properties of those PEI/DNA complexes, AFM was used to reveal the actual image of those complexes. In contrast to photon correlation spectroscopy measures was the hydrodynamic diameter of the particle in a specific solution, the intention of utilizing AFM was to measure the particle size of the PEI/DNA complexes more accurate. It is known that the hydrodynamic diameter determined by photon correlation spectroscopy varies with the thickness of the electrical double layer of

the particle, which is influenced by the ionic strength of the solution. AFM will, however, provide us the actual topography of the sample surface. Similar technique was utilized by several other researchers [22, 52-56]. The potential problem with AFM is that since all the samples were imaged in dry state instead of in solution, we need to justify that the particles were not generated as a result of drying, rather they were already formed in the solution prior to drying.

Our first approach in this study is imaging naked plasmid DNA alone. In this case, rodlike structures were observed from AFM images for both samples in H_2O and 3 mM NaCl (Figure 3-12). There was little evidence of intermolecular contacts because of the repulsive force between negatively charged DNA. The presence of NaCl in the solution did not affect the plasmid DNA in terms of shape and chain width, but intramolecular contacts were observed as suggested by the intramolecular loops. Also noticeably more DNA chains were observed under AFM. These results confirmed that charge shield effect of DNA molecules by higher ionic strength promoting the attachment of the sample to the mica surface.

PEI was then added to condense the rodlike DNA molecules. A kinetic study was then performed to investigate the process of PEI/DNA complexation. Cationic polymer was found to neutralize DNA, therefore dramatically reduced the repulsive force between DNA molecules, causing multi-molecular complexes to appear (Figure 3-13A). Under this condition, it was almost impossible to distinguish one DNA molecule from another. This finding implied that PEI/DNA complexes which formed later on were more likely to contain multiple DNA molecules instead of just one. Such observation correlated well with the polydispersity of PEI/DNA complexes in both H_2O and 3 mM NaCl buffer in

AFM studies. After 10 minutes of mixing, DNA and PEI formed tadpole-shaped particles (Figure 3-13B). These particles were generally smaller than the final particles, and the width of the tail was similar to the width of the naked plasmid DNA molecule. Apparently, the complexation process was not finished and DNA molecules were not fully condensed under these conditions. Free DNA tails and PEI molecules kept the repulsive force between particles relatively low. As a result, particles were typically seen to stick to each other. After 30 minutes of mixing, globular particles were formed, and tails disappeared (Figure 3-13C). Some of the particles merged into each other to form larger particles of irregular shapes. Repulsive force between particles restored, so that there were less particles close to each other. The only difference between these three samples was the incubation time. Hence, this set of study clearly demonstrated that the PEI/DNA complexes obtained by AFM imaging technique were formed prior to the drying process. Similar characteristic shapes of DNA complexes were observed by other researchers [24].

Particle size is considered as one of the most important parameters determining the performance of the condensed DNA complexes in gene transfer. In the next step, PEI/DNA complexes were prepared at different PEI/DNA mass ratio, and their AFM images were compared in terms of particle size. At lower PEI/DNA mass ratios, there was insufficient PEI to neutralize the DNA molecule, leaving some of the DNA unbounded as shown in Figure 3-10A. The presence of unbounded DNA noticed here corresponded well with early zeta potential distribution results that there are multiple types of complex with different charges in the solution. In 3 mM NaCl, the change of particle size corresponded well to the change of particle size determined by dynamic light

scattering for PEI/DNA complexes in NaCl buffer (See Figure 3-8), where the largest particle size appeared when the PEI/DNA mass ratio was 0.5. The results of zeta potential measurement we obtained earlier are consistent to AFM findings. The reason for PEI/DNA complexes reach largest size at the mass ratio of 0.5 would be the zeta potential of the complexes was close to neutrality.

Up to this point, we had a more solid understanding of the complexation of DNA and PEI, and the correlation between particle size and zeta potential. Further attention needs to be paid in determining the relationship between particle size and transfection efficiency.

6. CONCLUSIONS

In this study, numerous biophysical properties of PEI/DNA complexes, including particle size, particle shape, zeta potential and zeta potential distribution were determined. The results are invaluable to the success of gene delivery by PEI-based carrier, and may be useful for other nonviral transfection methods as well.

In this study, PEI/DNA mass ratio, ionic strength and pH value of the solution were varied to investigate the effect of the zeta potential of the complexes. From this study, we could conclude that (1) high ionic strength adversely affected the binding between cationic polymer and DNA, and promoted aggregation of the particles in the solution; (2) the solution pH between 5.0-8.0 did not make a significant difference in terms of zeta potential, partially because of the complicated heterocoagulation phenomena in the solution. Zeta potential distribution analysis later confirmed that more than one kind of particles coexisted in some of the solutions.

From this study, a correlation between the zeta potential of PEI/DNA complexes and their particle size was developed. When the zeta potential of the system was close to zero, PEI effectively neutralized DNA and the particle size of the complexes was the largest. Particle sizes at either lower or higher than this PEI/ DNA mass ratio were significantly smaller. The interactions between particles were mainly electrostatic in nature. Therefore, a slightly excessive amount of cationic polymer was required to retain the repulsive force between particles.

The results of AFM imaging not only echoed the corresponding change in particle size with PEI/DNA mass ratio, but also revealed the shape of those PEI/DNA complexes

and plasmid DNA itself. From the kinetic study performed using AFM, we conclude that complex formation occurred within 10 minutes upon the mixing of plasmid DNA and cationic polymer and completed after 20-30 minutes. Multiple plasmid DNA might entangle with each other during this complexation process. As a result, the complexes would be inherently different in size, i.e. not all the large complexes were of aggregation.

7. FUTURE PROSPECTS

The ultimate goal of this research is to develop a series of gene carriers for optimal gene delivery results. This includes maximizing transfection efficiency, minimizing cytotoxicity and increasing targeting specificity of the gene delivery system. Our focus in this study was primarily on characterizing the particle size and zeta potential of one specific cationic polymer-based gene carrier to understand interactions of gene delivery systems. Future strategies include investigating in different gene carriers so that their biophysical properties can be compared. Gene transfection efficiency experiments also need to be conducted in order to correlate those biophysical properties with gene transfection performance. As soon as sufficient data are collected, we will be able to find an optimal carrier for each individual gene delivery application.

It was postulated that by adding specific peptide sequence or functional group onto cationic polymer chain, transfection efficiency would be enhanced. But this may not always be the case. By examining different formula of modified cationic polymer under AFM, we will be able to determine if large particle size plays any role in limiting the performance, and further optimize the size of the gene delivery system by modifying the formula. We also plan to investigate other candidates, e.g. PLL, for gene delivery. Particle size information obtained by AFM will definitely help evaluating these new candidates.

Our kinetic study of DNA/PEI complexation process revealed important information of the interactions between DNA molecules and cationic polymers. However, it was limited by the time points we chose. Alternatively, we can image the samples in

solution under AFM. This way, real-time image will be obtained and it will help us understand the complete process of the interactions.

8. REFERENCE

1. Felgner, P.L., *Nonviral strategies for gene therapy.* Scientific American, 1997. **276**(6): p. 102.
2. Wyber, J.A., Andrews, J., and D'Emanuele, A., *The Use of Sonication for the Efficient Delivery of Plasmid DNA into Cells.* Pharmaceutical Research, 1997. **14**(6): p. 750-756.
3. Yang, N., Burkholder, J., Roberts, B., Martinell, B., and McCabe, D., *In vivo and in vitro gene transfer to mammalian somatic cells by particle bombardment.* Proceedings of the National Academy of Sciences USA, 1990. **87**(24): p. 9568–9572.
4. Wells, J.M., Li, L.H., Sen, A., Jahreis, G.P., and Hui, S.W., *Electroporation-enhanced gene delivery in mammary tumors.* Gene Therapy, 2000. **7**(7): p. 541–547.
5. Abdallah, B., Sachs, L., and Demeneix, B., *Non-viral gene transfer: Applications in developmental biology and gene therapy.* Biology of the Cell, 1995. **85**(1): p. 1-7.
6. Gershon, H., Ghirlando, R., Guttman, S.B., and Minsky, A., *Mode of formation and structural features of DNA-cationic liposome complexes used for transfection.* Biochemistry, 1993. **32**(28): p. 7143 - 7151.
7. Wu, G.Y., and Wu, C.H., *Receptor-mediated in vitro gene transformation by a soluble DNA carrier system.* Journal of Biological Chemistry, 1987. **262**(10): p. 4429-4432.
8. Zauner, W., Ogris, M., and Wagner, E., *Polylysine-based transfection systems utilizing receptor-mediated delivery.* Advanced Drug Delivery Reviews, 1998. **30**(1-3): p. 97-113.
9. Klevan, L. and Schumaker, V.N., *Stabilization of Z-DNA by polyarginine near physiological ionic strength.* Nucleic Acids Research, 1982. **10**(21): p. 6809-6817.
10. Wagner, E., Plank, C., Zatloukal, K., Cotten, M., and Birnstiel, M.L., *Influenza Virus Hemagglutinin HA-2 N-Terminal Fusogenic Peptides Augment Gene Transfer by Transferrin-Polylysine-DNA Complexes: Toward a Synthetic Virus-Like Gene-Transfer Vehicle.* Proceedings of the National Academy of Sciences USA, 1992. **89**(17): p. 7934-7938.
11. Rittner, K., Benavente, A., Bompard-Sorlet, A., Heitz, F., Divita, G., Brasseur, R., and Jacobs, E., *New Basic Membrane-Destabilizing Peptides for Plasmid-Based Gene Delivery in Vitro and in Vivo.* Molecular Therapy, 2002. **5**(2): p. 104-114.
12. Cho, Y.W., Kim, J.D., and Park, S.Y., *Polycation gene delivery systems: escape from endosomes to cytosol.* Journal of pharmacy and pharmacology, 2003. **55**(6): p. 721-734.
13. Haensler, J. and Szoka, F.C.Jr., *Polyamidoamine cascade polymers mediate efficient transfection of cells in culture.* Bioconjugate Chem., 1993. **4**(5): p. 372-379.
14. Boussif, O., Lezoualc'h, F., Zanta, M.A., Mergny, M.D., Scherman, D., Demeneix, B., and Behr, J., *A Versatile Vector for Gene and Oligonucleotide Transfer into*

Cells in Culture and in vivo: Polyethylenimine. Proceedings of the National Academy of Sciences USA, 1995. **92**: p. 7297-7301.

15. Suh, J., Paik, H.J., and Hwang, B.K., *Ionization of Poly(ethylenimine) and Poly(allylamine) at Various pH's.* Bioorganic Chemistry, 1994. **22**(3): p. 318-327.
16. Tang, M.X. and Szoka F.C., *The influence of polymer structure on the interactions of cationic polymers with DNA and morphology of the resulting complexes.* Gene Therapy, 1997. **4**(8): p. 823-832.
17. MacLaughlin, F.C., Mumper, R.J., Wang, J., Tagliaferri, J.M., Gill, I., Hinchcliffe, M., and Rolland, A.P., *Chitosan and depolymerized chitosan oligomers as condensing carriers for in vivo plasmid delivery.* Journal of Controlled Release, 1998. **56**(1-3): p. 259-272.
18. Funhoff, A.M., van Nostrum, C.F., Lok, M.C., Fretz, M.M., Crommelin, D.J.A., and Hennink, W.E., *Poly(3-guanidinopropyl methacrylate): A Novel Cationic Polymer for Gene Delivery.* Bioconjugate Chemistry, 2004. **15**(6): p. 1212-1220.
19. Gonzalez, H., Hwang, S.J., and Davis, M.E., *New Class of Polymers for the Delivery of Macromolecular Therapeutics.* Bioconjugate Chemistry, 1999. **10**(6): p. 1068-1074.
20. Bloomfield, V.A., *DNA condensation.* Current Opinion in Structural Biology, 1996. **6**(3): p. 334-341.
21. Choosakoonkriang, S., Lobo, B.A., Koe, G.S., and Middaugh, C.R., *Biophysical Characterization of PEI/DNA Complexes.* Journal of Pharmaceutical Science, 2003. **92**(8): p. 1710 – 1722.
22. Danielsen, S., Maurstad, G., and Stokke, B.T., *DNA-polycation complexation polyplex stability in the presence of competing polyanions.* Biopolymers, 2005. **77**(2): p. 86-97.
23. Bloomfield, V.A., *Condensation of DNA by multivalent cations: Considerations on mechanism.* Biopolymers, 1991. **31**(13): p. 1471-1481.
24. Maurstad, G., Danielsen, S., and Stokke, B. T., *Analysis of Compacted Semiflexible Polyanions Visualized by Atomic Force Microscopy: Influence of Chain Stiffness on the Morphologies of Polyelectrolyte Complexes.* Journal of Physical Chemistry B, 2003. **107**(32): p. 8172-8180.
25. Grosberg, A.Y., and Kuznetsov, D.V., *Quantitative theory of the globule-to-coil transition. 1. Link density distribution in a globule and its radius of gyration.* Macromolecules, 1992. **25**(7): p. 1970 - 1979.
26. Tang, M.X., and Szoka, F.C., *The influence of polymer structure on the interactions of cationic polymers with DNA and morphology of the resulting complexes.* Gene Therapy, 1997. **4**: p. 823-832.
27. Ivanov, V.A., Paul, W., and Binder, K., *Finite chain length effects on the coil–globule transition of stiff-chain macromolecules: A Monte Carlo simulation.* Journal of Chemical Physics, 1998. **109**(13): p. 5659–5669.
28. Park, S.Y., Harries, D., and Gelbart, W.M., *Topological defects and the optimum size of DNA condensates.* Biophysical Journal, 1998. **75**(2): p. 714-720.
29. Widom, J., and Baldwin, R.L., *Cation-induced toroidal condensation of DNA : Studies with Co3+(NH3)6.* Journal of Molecular Biology, 1980. **144**(4): p. 431-453.

30. Liu, G., Molas, M., Grossmann, G.A., Pasumarthy, M., Perales, J.C., Cooper, M.J., and Hanson, R.W. *Biological Properties of Poly-L-lysine-DNA Complexes Generated by Cooperative Binding of the Polycation.* The Journal of Biological Chemistry, 2001. **276**(37): p. 34379-34387.
31. Gershon, H., Ghirlando, R., Guttman, S.B., and Minsky, A., *Mode of formation and structural features of DNA-cationic liposome complexes used for transfection.* Biochemistry, 1993. **32**(28): p. 7143 - 7151.
32. Adami, R.C., Collard, W.T., Gupta, S.A., Kwok, K.Y., Bonadio, J., and Rice, K.G., *Stability of peptide-condensed plasmid DNA formulations.* Journal of Pharmaceutical Sciences, 1998. **87**(6): p. 678-683.
33. Florea, B.I., Meaney, C., Junginger, H.E., and Borchard, G., *Transfection Efficiency and Toxicity of Polyethylenimine in Differentiated Calu-3 and Nondifferentiated COS-1 Cell Cultures.* AAPS PharmSci, 2002. **4**(3): p. 1-11.
34. Dunlap, D.D., Maggi, A., Soria, M.R., and Monaco, L., *Nanoscopic structure of DNA condensed for gene delivery.* Nucleic Acids Research, 1997. **25**(15): p. 3095-3101.
35. Kircheis, R., Wightman, L., and Wagner, E., *Design and gene delivery activity of modified polyethylenimines.* Advanced Drug Delivery Reviews, 2001. **53**(3): p. 341-358.
36. Ogris, M., Steinlein, P., Kursa, M., Mechtler, K., Kircheis, R., and Wagner, E., *The size of DNA/transferrin-PEI complexes is an important factor for gene expression in cultured cells.* Gene Therapy, 1998. **5**(10): p. 1425-1433.
37. Ahn, C.H., Su, Y.C., You, H.B., and Sung, W.K., *Biodegradable poly(ethylenimine) for plasmid DNA delivery.* Journal of Controlled Release, 2002. **80**(1-3): p. 273-282.
38. Ogris, M., Brunner, S., Schüller, S., Kircheis, R., and Wagner, E., *PEGylated DNA/transferrin-PEI complexes: reduced interaction with blood components, extended circulation in blood and potential for systemic gene delivery.* Gene Therapy, 1999. **6**(4): p. 595-605.
39. Kircheis, R., Wightman, L., Schreiber, A., Robitza, B., Rössler, V., Kursa, M., and Wagner, E., *Polyethylenimine/DNA complexes shielded by transferrin target gene expression to tumors after systemic application.* Gene Therapy, 2001. **8**(1): p. 28-40.
40. Wightman, L., Kircheis, R., Rössler, V., Carotta, S., Ruzicka, R., Kursa, M., and Wagner, E., *Different behavior of branched and linear polyethylenimine for gene delivery in vitro and in vivo.* Journal of Gene Medicine, 2001. **3**(4): p. 362-372.
41. Akinc, A., Lynn, D.M., Anderson, D.G., and Langer, R., *Parallel synthesis and biophysical characterization of a degradable polymer library for gene delivery.* Journal of the American Chemical Society, 2003. **125**(18): p. 5316-5323.
42. Munier, S., Messai, I., Delair, T., Verrier, B., and Ataman-Onal, Y., *Cationic PLA nanoparticles for DNA delivery: Comparison of three surface polycations for DNA binding, protection and transfection properties.* Colloids & Surfaces B: Biointerfaces, 2005. **43**(3-4): p. 163-173.
43. Liu, J., Zhou, Z., Xu, Z., and Masliyah, J., *Bitumen–Clay Interactions in Aqueous Media Studied by Zeta Potential Distribution Measurement.* Journal of Colloid and Interface Science, 2002. **252**(2): p. 409-418.

44. Park, S.Y., Harries, D., and Gelbart, W.M., *Topological Defects and the Optimum Size of DNA Condensates.* Biophysical Journal, 1998. **75**(2): p. 714-720.
45. Binnig, G.B., Quate, C.F., and Gerber, C., *Atomic Force Microscope.* Physical Review Letters, 1986. **56**(9): p. 930-933.
46. Mel'nikova, Y.S. and Lindman, B., *pH-Controlled DNA Condensation in the Presence of Dodecyldimethylamine Oxide.* Langmuir, 2000. **16**: p. 5871-5878.
47. Chen, K.M., Jiang, X., Kimerling, L.C., and Hammond, P.T., *Selective Self-Organization of Colloids on Patterned Polyelectrolyte Templates.* Langmuir, 2000. **16**: p. 7825-7834.
48. Oupicky, D., Konak, C., Ulbrich, K., Wolfert, M.A., and Seymour L.W., *DNA delivery systems based on complexes of DNA with synthetic polycations and their copolymers.* Journal of Controlled Release, 2000. **65**(1-2): p. 149-171.
49. Oupicky, D., Konak, C., and Ulbrich, K., *Preparation of DNA complexes with diblock copolymers of poly [N(2-hydroxypropyl)methacrylamide] and polycations.* Materials Science & Engineering C-Biomimetic and Supramolecular Systems, 1999. **7**(1): p. 59-65.
50. Le-Pecq, J.B., and Paoletti, C., *A fluorescent complex between ethidium bromide and nucleic acids.* Journal of Molecular Biology, 1967. **27**: p. 87-106.
51. Godbey, W.T., Wu, K.K., and Mikos, A.G., *Size matters: Molecular weight affects the efficiency of poly(ethylenimine) as a gene delivery vehicle.* Journal of Biomedical Materials Research, 1999. **45**: p. 268-275.
52. Danielsen, S., Vårum, K.M., and Stokke, B.T., *Structural Analysis of Chitosan Mediated DNA Condensation by AFM: Influence of Chitosan Molecular Parameters.* Biomacromolecules, 2004. **5**(3): p. 928-936.
53. Merdan, T., Kunath, K., Petersen, H., Bakowsky, U., Voigt, K.H., Kopecek, J., and Kissel, T., *PEGylation of poly(ethylene imine) affects stability of complexes with plasmid DNA under in vivo conditions in a dose-dependent manner after intravenous injection into mice.* Bioconjugate Chemistry, 2005. **16**(4): p. 785-792.
54. Wang, C.H. and Hsiue, G.H., *Polymer-DNA hybrid nanoparticles based on folate-polyethylenimine-block- poly(L-lactide).* Bioconjugate Chemistry, 2005. **16**(2): p. 391-396.
55. Petersen, H., Merdan, T., Kunath, K., Fischer, D., and Kissel, T., *Polyethylenimine-graft-Poly(ethylene glycol) Copolymers: Influence of Copolymer Block Structure on DNA Complexation and Biological Activities as Gene Delivery System.* Bioconjugate Chemistry, 2002. **13**(4): p. 812-821.